UNIVERSITY OF THE PHILIPPINES

DYNAMICS OF AN SIS-LIKE AUDIENCE APPLAUSE MODEL

by

ANTONIO MIGUEL V. CRUZ

An Undergraduate Thesis submitted to the
National Institute of Physics
College of Science
University of the Philippines
Diliman, Quezon City

In Partial Fulfillment of the Requirements
for the Degree of
Bachelor of Science in Applied Physics

Date of Submission:
June 2018

Thesis Classification:
F

This thesis is available to the public.

ABSTRACT

DYNAMICS OF AN SIS-LIKE AUDIENCE APPLAUSE MODEL

Antonio Miguel V. Cruz
University of the Philippines (2018)

Adviser:
Johnrob Y. Bantang, Ph.D.

The audience applause is a social phenomena that is very rich in dynamics. This human behavior is a collective of interacting agents that can be treated as a complex system. Studies have treated the audience applause similarly to a disease in order to apply epidemic models to analyze the dynamics. A compartmental SCS model based on the SIS epidemic model is created and simulated using the Monte Carlo method where state transitions S $\rightarrow$ C $\rightarrow$ S. Functions are included in order to reproduce the audience applause as accurately as possible. f is a forcing function that initiates the state transitions. $f'(\alpha)$ is a feedback function that promotes agents to transition to state C if more agents are in state C. $g'(\beta)$ is a modulation function that inhibits agents in state C to transition to state S. Simulations with specific parameter sets (a, b, α, β) show cases where the state n_c never reaches zero, or that the applause never ends (which doesn't occur in real life). The steady-state of the system is calculated and plotted in phase space in order to analyze its dynamics. For $\beta \leq 1$, there are two solutions, the trivial ($n_c^\infty = 0$), and non-trivial steady-state ($n_c^\infty > 0$). For $\beta > 1$, there are three solutions, the trivial solution, and two non-trivial solutions. These two solutions are the upper branch ($n_{c1}^\infty > 0$) and the lower branch of the curve ($n_{c2}^\infty > 0$). Critical points have been observed to which the system experiences bifurcation from the trivial steady-state to the non-trivial steady-state. For parameter sets with $\beta > 1$, the lower branch was shown to be unstable. If the system starts in state n_c with $\bar{a}$ values on the lower branch of the curve, it can settle to either trivial or non-trivial solution. The original SCS model exhibited scale-free behavior when the population size was increased. Spatial effects were incorporated to the SCS model in order to more appropriately model the audience applause. This is then confirmed by comparing with a real-life applause data set.

PACS: 02.50.Ey Stochastic processes, 87.10.Rt Monte Carlo simulations, 89.65.-s Social and economic systems

Table of Contents

List of Figures

Chapter 1

Applause Dynamics

1.1 Nature of Applause

The audience applause is one of the most ubiquitous and timeless social phenomenons observed in human culture. People would normally applaud to express their approval over a social event, and may even jeer, shout, snap, and boo, on top of clapping. People collectively seem to know when to start clapping in any occasion, whether it is during or after a speech, performance, sport event, etc. People also unconsciously know whether to continue clapping or to stop. Audience members extend their applause to musicians playing an outro or to being addressed, and stop immediately when the musician proceeds with the next song. Lastly, it is historically known that people who have been hired to willingly and consciously applaud are inserted in an audience in hopes to extend the applause for a social event [1]. These observations of an audience applause being self-organized and somehow connected give rise to the question of what the social dynamics are among the audience and they decide when and how long to clap.

1.2 Social Dynamics

Social economics is an interdisciplinary study of the interrelationship between group and individual behavior. Individual decisions made interactively with others have been modeled formally to be able to understand the dynamics of the system. The underlying assumption is that individuals are influenced by the choices of others. From this assumption, it can be said that feedback loops exist since the past decisions of a certain individuals may influence future decisions of others. Examples of such social phenomena are crime, teenage pregnancy, and high school dropout rates.[2][3]

Tools that can be used to quantify and analyze the dynamics are network theory and complex systems.

1.3 Quantifying the Dynamics

1.3.1 Networks

A network is a collection of points,called vertices or nodes, connected by lines, called edges. Networks are normally used to represent systems that contain individual parts that are somehow connected, such as the internet, big data, or social interactions [4]. These are used to study the nature of individual components and their dynamics. A few properties of networks are topology and homogeneity. Network topology refers to how the network is connected. The different topologies are named after the physical shape of the network, such as a ring or a line. A key topology is a fully-connected network wherein all nodes are completely connected to each other[5]. Network homogeneity refers to the nodes of the network. A homogeneous network has individual nodes of the same characteristics and properties while a heterogeneous network contains different nodes.

1.3.2 Complex Systems

By investigating the mechanisms that determine the topology of the networks of aforementioned systems (internet, big data, etc.) properties previously not observed when studying the components individually emerge. This has lead to a new field of study that focuses on how relationships between components give rise to its collective behaviors and how the system interacts and forms relationships with its environment, called complex systems. Intrinsic to complex systems is that they are hard to model due to the complexity of the interacting components. Over-simplifying the complexity may lead to the failure of the model[6]. Included in as a property of complexity is the inclination of a large system to mutate after reaching a critical point or state. Methods on studying complex systems have been established and broken down to three parts, data acquisition, modelling, and measuring complexity. Data acquisition generally tends towards statistical learning and data mining. Modelling turns to mainly two methods, cellular automata and agent-based modelling[7]. Measuring complexity has demanded an inclusion of new metrics. These metrics include average path length,

clustering coefficient, degree distribution, and spectral properties[8].

1.3.3 Cellular Automata

The cellular automata is a simple mathematical model used to investigate self-organization in statistical mechanics. This model represents spatial dynamics and highlights local interactions, spatial heterogeneity, and large-scale aggregate patterns. The simplest model arranges the agents in a grid. From here agents interact with each other according to certain specified rules. Interaction among agents varies upon the prescribed neighborhood. One neighborhood in particular is the Moore neighborhood. This takes all adjacent spaces in all directions (N,S,E,W,NE,NW,SE,SW) from a reference agent. An extended Moore neighborhood extends the interactions n units away from the reference agent. A modified Moore neighborhood changes the interactable directions [9].

1.4 The audience as a complex system

Human behavior is usually studied qualitatively (under psychology or sociology) and is notoriously hard to quantify due to all the possible parameters and the difficulty in creating a controlled environment. The audience applause is an example of human behavior that is a collective of interacting agents with underlying dynamics. This allows us to treat the audience as a complex system in order to study its complexity and dynamics.

1.5 Known Studies and Models

There have been very little studies made on applause, down to the sound [10], its rhythm [11] and its dynamics [12]. One particular study treats the applause as a contagion that propagates through the audience, allowing it to be modelled using an SIR-model. The SIR-model allows each unit in the model (for this case, each person henceforth referred to as an agent) to have 3 states, susceptible, infected, and recovered. Each agent is initially silent before the applause (susceptible). After which they start to applaud (infected). Finally stop clapping (recovered). Such a model would be appropriate if the agents no longer clap again after stopping, but cases exist where the agent my stop clapping prematurely, and then feel obliged to clap again due

to the fact that the rest still continue to do so. With that, an SIS-like compartmental model with only two states(susceptible or infected) is adapted to properly account for such cases.

1.6 Problem Statement

The dynamics of the applause of an audience with N agents using an SIS epidemic model is presented and analyzed. The agents are connected via two dimensional lattice network and are initially fully connected. Later on, the agents will observe a modified, extended Moore neighborhood in order to incorporate spatial effects. The network is assumed to be homogeneous for simplicity; all agents share the same parameters for a given simulation. Agents are assumed to clap immediately after a performance, and may continue to do so depending on their given parameters. The dynamics of the system are also analyzed. Spatial effects are then incorporated to the model to more appropriately simulate audience applause. This is done to investigate if there is a correlation between the applause duration and the audience size. The simulations will also be confirmed with a dataset of real-life applause. Why people applaud and to what are not investigated due to its unquantifiable nature.

Chapter 2

Monte Carlo Compartmental Method

Modelling epidemics has been done in order to study the mechanisms by which diseases spread. This helps in predicting how fast and far the disease can spread in order to control and prevent future outbreaks [13]. By treating the applause similarly to a disease that spreads in the audience, the same tools to model epidemics can be used to model the applause [12].

2.1 Compartmental Model

2.1.1 States

The proposed compartmental model separates the agents into two states, silent (S) and clapping (C). The silent state replaces the susceptible state while clapping state replaces the infected state. Intuitively, agents in state S are audience members who are not clapping while agents in state C are audience members who are clapping. The number of agents in state S, given by n_s, and the number of agents in state C, given by n_c, dictate the state of the system, given by $\vec{n}$ where $\vec{n} \equiv (n_c, n_s)$. It is assumed that the total number of agents N is fixed, where $N = n_c + n_s$ and $\vec{n}$ is fully specified by n_c alone.

2.1.2 Parameters

The parameters a and b are the transition parameters. They range from 0 to 1 to represent transitional probabilities. The transitional probabilities from S to C and C to S are controlled by a and b respectively. The corresponding transition probabilities

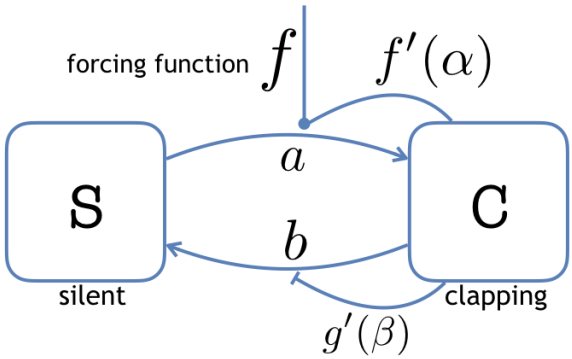

Figure 2.1: The compartmental model of audience applause based on the SIS epidemic model. Agents are either in state S or state C. Parameters a and b are the transitional probabilities. Functions f, f', and g' are further discussed.

are given by R_1 and R_2 where

$$\mathrm{R}_1 \quad : \quad \mathrm{S} \xrightarrow{a} \mathrm{C} \tag{2.1}$$

$$\mathrm{R}_2 \quad : \quad \mathrm{C} \xrightarrow{b} \mathrm{S}. \tag{2.2}$$

2.1.3 Functions

An audience is initially silent until given a social cue to start clapping, such as the end of a performance. This corresponds in the model to all agents starting in state S, and then forcing the agents to undergo R_1. The function f forces the transition R_1 for an indicated time interval, τ, which is typically 2-3 seconds/iterations. Once f expires, the system behaves freely and its agents may undergo various R_1 and/or R_2 transitions depending on the given parameters.

Aside from social cues, audience members may start clapping simply because others are. The peer influence may cause agents unaffected by social cues to start clapping, or those who have already stopped clapping to clap again. This creates a feedback mechanism that initiates more people to clap if majority of the agents are clapping corresponding in the model to the function f'. The function f' incorporates this feedback mechanism and is parametrized by α:

$$f'(\alpha) = \alpha \frac{n_c}{N-1}, \tag{2.3}$$

where α ranges from 0 to 1 for probabilistic interpretations. The probability for a spontaneous R_1 transition is directly proportional to α and the fraction of the population in state C. The denominator is set to $N-1$ because an agent cannot

spontaneously influence itself; it is only influenced by the rest of the population. The function is more effective when there are more agents in state C.

Finally, audience members may contain their own bias towards a social event and may applaud longer or shorter depending on the bias. Also, the continuous applause of the majority can inhibit those who are clapping to stop clapping. This corresponds in the model to the function g'. The factor g' incorporates the inhibition as a modulation function and is parametrized by β:

$$g'(\beta) = \frac{1}{1 + \beta\ n_C/(N-1)} \tag{2.4}$$

where $\beta \geq 0$, representing the bias. Higher β translates to agents less likely to undergo transition R_2 Equation (2.4) is taken from the Michaelis-Menten equation, which aims to model enzyme kinetics[14]. Figure 2.1 shows how the states and functions interact to complete the compartmental SCS model.

This completes the differential equations for the reactions (2.1) and (2.2):

$$\frac{d}{dt}n_c = a(f + f' - f'f)n_s - bg'n_c \tag{2.5}$$

$$\frac{d}{dt}n_s = bg'n_c - a(f + f' - f'f)n_s \tag{2.6}$$

These equations are consistent with the assumption that the total audience size is fixed, that is $dn_c/dt = -dn_s/dt$. The derivation for the combined probability of the functions f and f' is shown in Appendix A.

2.2 Simulation Alogrithm

The compartmental SIS-like model is confirmed by simulating the R_1 and R_2 process via an agent-based Monte Carlo method. For each iteration, every agent is assigned a random number that is compared to one of the transition probabilities:

$$P(\mathrm{R}_1) = a(f + f' - f'f) \tag{2.7}$$

$$P(\mathrm{R}_2) = bg' \tag{2.8}$$

Agents in state S undergo transition R_1 with probability shown in (2.7). Agents in state C undergo transition R_2 with probability shown in (2.8). A uniform random number, u, where $u \in [0, 1]$, is drawn from a random number generator and then

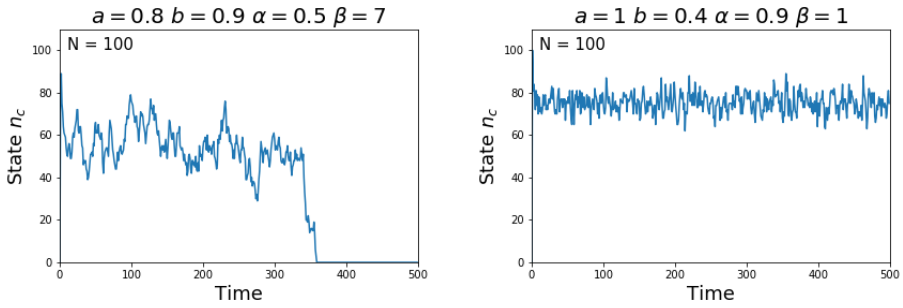

(a) A simulation with finite applause time.

(b) A simulation that seams to oscillate in a certain value.

Figure 2.2: Sample simulations given a fixed population $N = 100$. Simulation (a) is a typical, intuitive audience applause that has an end. Simulation (b) is non-trivial and counter-intuitive in that it seems to have no end.

compared to the corresponding probability P. If $u \leq P$, the appropriate transition is allowed to occur.

The simulator outputs a graph of n_c versus time, where time is defined to be each iteration. Examples of such simulations are shown in figure 2.2. An emergent property of the system is that a certain set of parameters will simulate an audience applause that does not end. Even if such cases do not exist in real life, further investigation of the steady-state applause may unravel the complexity of the system.

Chapter 3

Steady-state dynamics of the audience applause

A system is in steady-state when its behavior no longer changes in time. In the context of a real audience applause, the system rapidly spikes up in the number of people applauding, fluctuates, then slowly dies down till everyone stops clapping. This setup has the trivial steady-state of 0. However, simulations have shown that there are parameters where the steady-state is not zero, corresponding to n_c people clapping indefinitely. The value can be calculated by equating either (2.5) or (2.6) to zero, plugging in the given parameters a, b, α, β, and then solving for n_c.

3.1 Steady-state equation for different cases

The steady-state conditions are when the state $\vec{n}$ is fixed and when the forcing function expires. This is when $d\vec{n}/dt = 0$ and when $f = 0$. The derivation is shown in the appendix (B) Once these conditions are achieved, (2.5) and (2.6) are simplified to the steady-state equation for n_c

$$\bar{a}(N - n_c)(N - 1 + \beta n_c) = b(N - 1)^2 \tag{3.1}$$

where $\bar{a} \equiv a\alpha$. The values of steady state n_c may be solved for any given $\bar{a}, b$, and β. Parametrizing (3.1) to time gives the phases space plot for the given parameters b and β, shown in figure 3.1. The phase space plots of the analytical steady-state values for various b values are shown in Appendix C. Though the trivial steady-state solution is not included in (3.1), it has been included in the phase space. The coordinate ($\bar{a}$,n_c) on the curves represent the n_c value for a given $\bar{a}$ value at the given b and β value. The different colors for the curves correspond to the different β values as

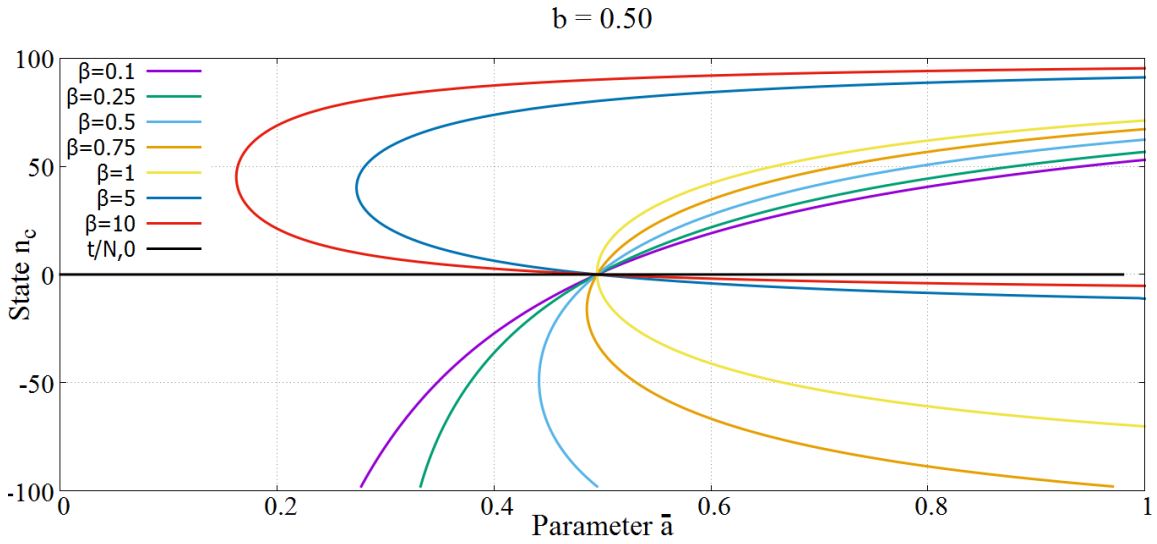

Figure 3.1: The phase space plot of the analytical steady-state value n_c versus $\bar{a}$ for various β values and $b = 0.5$. Included is the trivial steaty-state solution $n_c = 0$

shown in the legend. Values below 0 are extraneous since n_c refers to the number of people clapping, which cannot be negative. This means that there are two possible steady-state values for $\beta \leq 1$, the trivial solution 0, and the non-trivial solution found on the appropriate curve. On the other hand, there are three possible steady-state values for $\beta > 1$, the trivial solution 0, and two non-trivial solutions found on the appropriate curve.

3.1.1 Bifurcation Theory

Given a specific parameter set (a, b, α, β), the steady-state solution can only either be the trivial (0, in black) or non-trivial, never both. How this is determined falls under bifurcation theory. This refers to the study of change to the state of the system as a parameter or parameters are changed and can be applied to steady-state systems [15]. The system is analyzed to find out where the change occurs and if there are stability changes.

3.1.2 Critical Points

From observing all phase space plots of various b values, all β curves intersect, along with the trivial solution, at a specific point. Setting $n_c = 0$ in (3.1) gives us this critical point of intersection, $\bar{a}_1$:

$$\bar{a}_1 = \frac{b(N-1)}{N} \tag{3.2}$$

which for $N \gg 1$ results to the observed $\bar{a}_1 \approx b$. Solution for the critical point is shown in Appendix D

The non-trivial solution to the steady-state equation (3.1) is quadratic, which does not include the trivial solution. This results to two non-trivial n_c solutions for a given $\bar{a}$. For $\beta \leq 1$, the non-trivial steady-state solutions appear uniquely for $\bar{a} > \bar{a}_1$ since the second n_c value is negative and therefore, extraneous. However, when $\beta > 1$, two non-trivial solutions appear between a new critical value of $\bar{a} = \bar{a}_2$, corresponding to the vertex of (3.1), and $\bar{a}_1$. For $\bar{a} > \bar{a}_1$, the non-trivial steady-state solution appears uniquely once again, similar to $\beta \leq 1$. The $\bar{a}_2$ is given by

$$\bar{a}_2 = \frac{b(N-1)^2}{(N-n_c^*)(N-1+\beta n_c^*)} \tag{3.3}$$

where $n_c^* \equiv [1 + (\beta - 1)N]/2\beta$. Derivation is shown in the appendix (D This non-trivial solution however, is unstable upon substitution with $\ddot{\vec{n}}$ resulting to $\ddot{\vec{n}} < 0$. Thus, the middle branch in the range $\bar{a} \in (\bar{a}_2, \bar{a}_1)$ is an unstable steady-state.

3.2 Simulation experiments

Analytical results are confirmed by simulation. The number of iterations, t, is set to be much greater than the duration of the forcing function,τ. Figure 3.2 shows sample simulations along with the analytical steady-state and the average of the system. The analytical steady-state is plotted in green while the mean is plotted in red. As observed, the simulation closely resembles the analytical value. The system settles to its steady-state very early in the simulation since it starts to oscillate around the steady-state neat $t = 0$. It can be safely assumed that the n_c values at $t \gg \tau$ are equivalent to n_c for $t \to \infty$.

Ten sample runs were performed with different initial random number generator states and the final n_c value for each iteration were recorded. The mean and standard deviation of the simulated steady-state values are then computed for each parameter space $(\bar{a}, b, \beta)$. The data points were then plotted with the corresponding parametrized differential curve shown in Fig. 3.3. More simulation experiments for various b values are shown in Appendix E

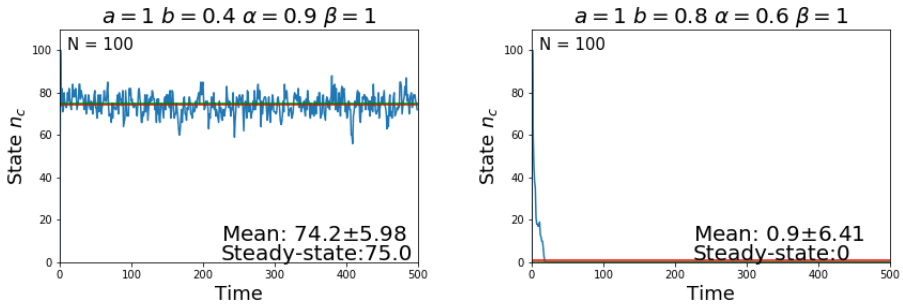

(a) A simulation with a steady state of 75. The average n_c is close to the analytic value.

(b) A simulation with a steady state of 0. The average n_c value is approximately 0.

Figure 3.2: Sample simulations that compare the analytical steady-state of the given parameters and the mean n_c value of the system. In green is the analytical steady-state value. In red is the mean n_c of the system.

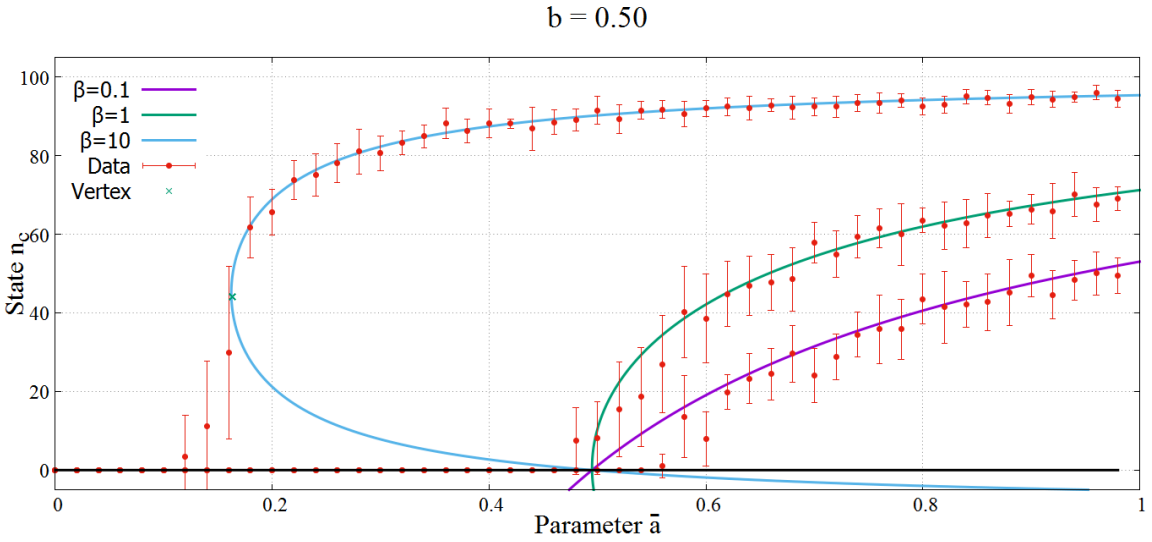

Figure 3.3: The simulated steady-state values plotted against the analytic steady-state curves. The error bars provide the extent of deviation in simulations. The vertex is represented with the cross.

For $\beta \leq 1$, the simulation is consistent with the trivial steady state solution until it reaches the critical point $\bar{a} = b$, after which follows non-trivial, non-extraneous solution consistent with (3.1). Bifurcation occurs at $\bar{a}_1$. For $\beta > 1$, the simulation follows the trivial steady-state and then breaks away and approaches the vertex of (3.1) at $\bar{a}_2$, after which, continues to follow the upper branch of (3.1). Bifurcation occurs somewhere before $\bar{a}_2$ The analytical solutions fail to predict the bifurcation from the trivial solution to the vertex of the curve. Also, the significance of the lower branch for $\beta > 1$ curves is unknown and warrants further investigation.

3.2.1 Unstable points

For the previous simulation experiments, all agents start at state S and then forced to transition to state C. To investigate the properties of the lower branch on the non-trivial solution, we vary the number of agents that start the simulation in state C and remove the forcing function. This allows us to determine where the system will settle given the specific starting n_c value, more particularly for n_c values near the lower branch of the non-trivial solution.

Shown in figure 3.4 are the new phase space graphs that include arrows that point to where that n_c value for the given $\bar{a}$ settles. More vector graphs are available in Appendix F The color of the arrows represents the probability of going towards that direction. Intuitively for $\beta \leq 1$, all n_c values point towards the trivial solution for all $\bar{a}$ values less than $\bar{a}_1$ 100% of the time. All n_c with $\bar{a}$ values greater than $\bar{a}_1$ point towards the non-trival solution 100% of the time. For $\beta > 1$, what differs is the behavior at the vertex and the lower branch of the non-trivial solution. Points with n_c values above the vertex have an estimated 50% to either settle at the vertex or zero, while n_c values below the vertex absolutely settle to zero. Points slightly above the lower branch tend to settle towards the upper branch more but still have a chance to settle at 0. The same can be said for points below the lower branch. Points within the lower branch have a 50% of settling to either trivial or non trivial solution. This means that coordinates near the lower non-trivial branch are unstable, since there is no certainty to which steady-state solution they will settle to.

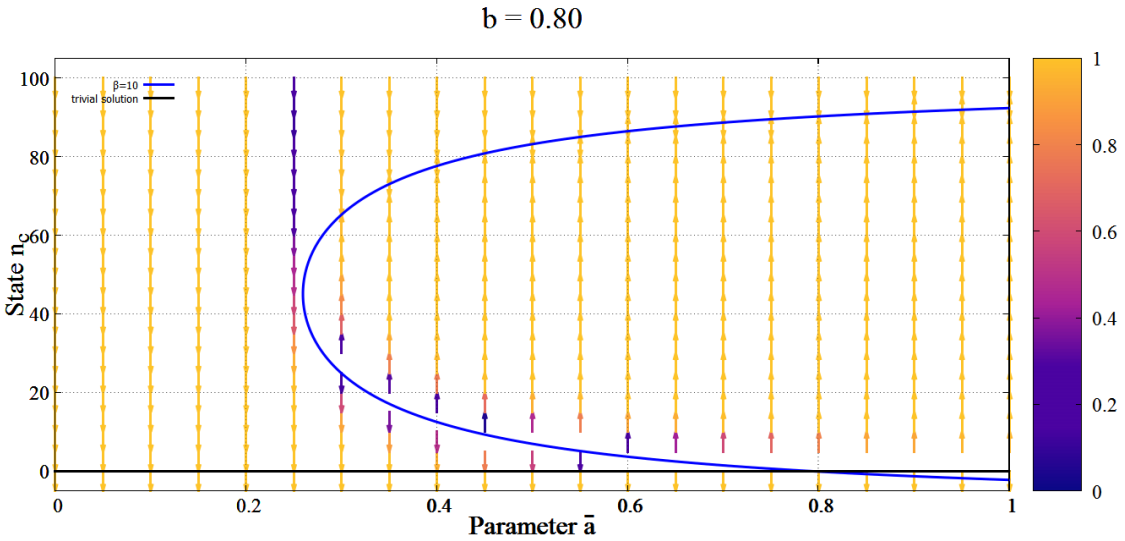

Figure 3.4: Vector graph for parameters $b = 0.8, \beta = 10$. The origin of the vector represents the initial n_c and corresponding $\bar{a}$ value. The direction it points reveals whether it settles to the trivial or non-trivial solution. The color represents the probability of settling towards the directed steady-state.

Chapter 4

Incorporating Spatial Effects

After analysing the model, it was then compared to real applause. The applause duration of varying audience sizes were taken from Youtube videos of musical concerts and performances. The applause duration was manually recorded. The audience size was either taken from the seating capacity and/or ticket sales for the given concert/performance, or was estimated by the area or room the audience resided in. The relationship of the data set was tested with both applause duration and population size in order to find an appropriate linear dependence, as shown in figure 4.1.

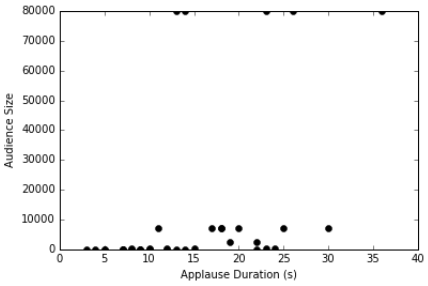

(a) Graphing size versus applause duration.

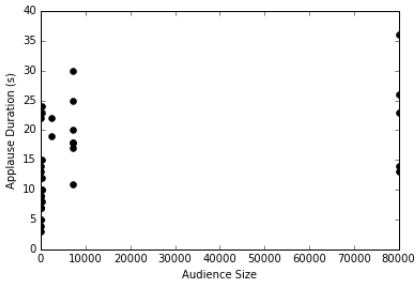

(b) Graphing applause duration versus size.

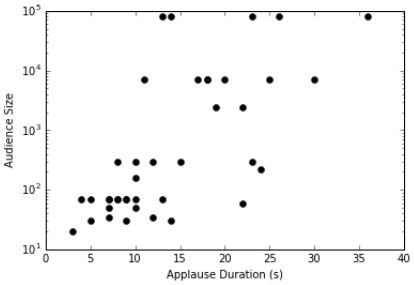

(c) Graphing size (in the logarithmic scale) versus applause duration

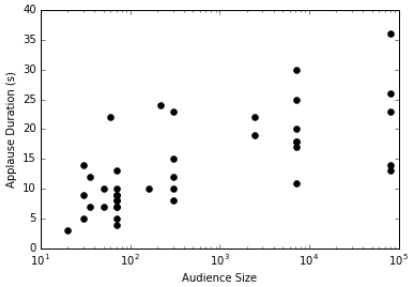

(d) Graphing applause duration versus size (in the logarithmic scale).

Figure 4.1: Different graphs of the data points of real-life applause.

Figure 4.1 (d) makes the most sense; the applause duration of the audience is dependent on the size of the audience. The question now is whether or not the compartmental model can recreate 4.1 (d). The current model shows no population size dependence; changing the population size does not affect the applause duration for a given set of parameters. This is because of the assumption that the network is fully connected, meaning that an audience member in front is influenced the exact same way by the whole audience as an audience member at the back. As this does not seem to be the case in real-life applause, spatial effects must be incorporated by modifying the feedback function $f'(\alpha)$.

4.1 Different configurations for field of vision

The field of view configurations represent the audience members that may influence the reference agent. In real life, the reference agent is influenced by a limited number of audience members, not the whole audience. The network is no longer fully-connected, observing a modified, extended Moore neighborhood. It is extended since it considers all agents till the front row of the system, and not just those 1 unit away. It is modified since it does not consider all directions; the directions considered are affected by the configuration. $\theta = 0$ represents all audience members only directly in front of the reference agent until the very front. $\theta = \pi$ represents all rows ahead of the reference agent. $\theta = \frac{\pi}{2}$ considers all agents from the north-east direction to the north-west in a 90 degree arc. The configurations are shown in figure 4.2.

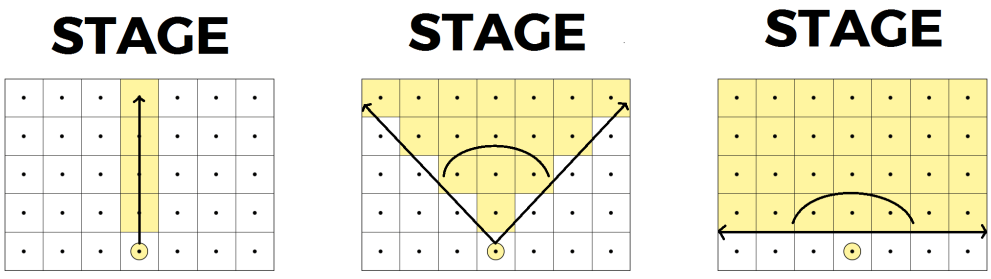

(a) $\theta = 0$ (b) $\theta = \frac{\pi}{2}$ (c) $\theta = \pi$

Figure 4.2: Different field-of-view configurations. The encircled black dot shaded in yellow is the reference agent. The boxes highlighted in yellow are what can influence the encircled reference agent.

4.2 Simulating the different spatial configurations

Initially, $f'(\alpha)$ bases the fraction of n_c throughout the whole population. After incorporating spatial effects, that fraction is only within the field-of-view of the reference agent. The feedback function is still parametrized by α.

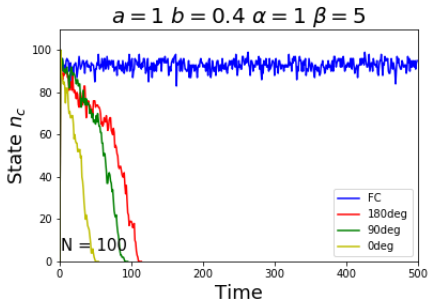

(a) Comparing simulations with spatial effects to the original fully-connected simulation.

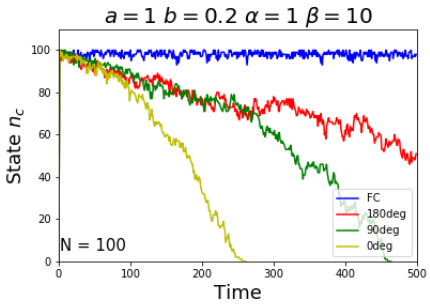

(b) $\theta = 180$ has yet to reach steady-state but is steadily heading towards 0.

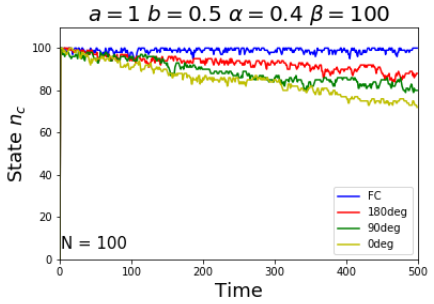

(c) All simulations are slowly reaching steady-state.

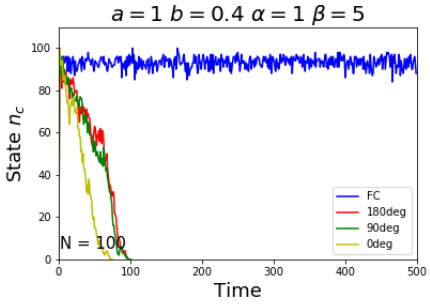

(d) A case where $\theta = \frac{\pi}{2}$ is similar to $\theta = 0$.

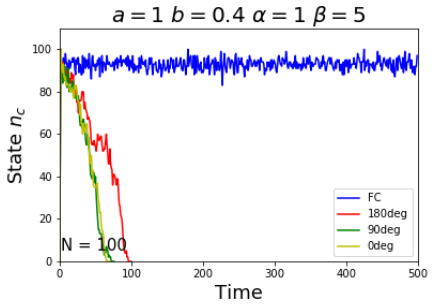

(e) A case where $\theta = \frac{\pi}{2}$ is similar to $\theta = \pi$.

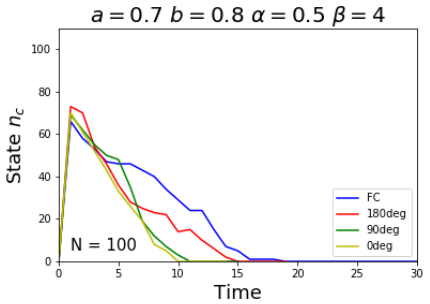

(f) All configurations have a trivial steady-state 0.

Figure 4.3: Different graphs comparing effect of different feedback functions under different parameters.

Shown in figure 4.3 are simulations with different parameters (a, b, α, β) comparing the different feedback functions, the original fully-connected network, $\theta = \pi$, $\theta = \frac{\pi}{2}$, and $\theta = 0$. Graphs (a), (b), and (c) show that in our system, feedback functions

are less effective in less connected networks. There is clearly a downward trend when it comes to applause duration. Graphs (d) and (e) show that $\theta = \frac{\pi}{2}$ can be similar to either remaining configurations, as well as be somewhere in between. Generally, simulations incorporating any form of field-of-view feedback do not have a non-trivial steady-state. Graphs (b) and (c) show cases where the simulations have not ended, but exhibit an obvious downward trend. Given more iterations, the simulations would end, unlike the fully-connected ones. Graph (g) shows a special case where all simulations have a trivial steady-state of zero. One thing to note is that the analysis done for the fully-connected system (phase space graphs, critical and unstable points) cannot be applied to the systems with spatial effects. A different steady-state equation must be setup to reflect how each agent is influenced differently. Such analysis will no longer be pursued as it is outside the scope of the study.

4.3 Finding the parameters (a, b, α, β) for real-life applause

Recalling, incorporating spatial effects to the feedback function effectively reduces the number of agents influencing a reference agent. Increasing the population size should increase the feedback since the agents in the back row of a 100x100 grid should 'see' more people than those in the back row of a 10x10 grid. This effectively eliminates the original problem of the fully-connected network being scale free. It is now possible for the applause duration to be dependent on the population. This phenomena is investigated by simulating a set of parameters (a, b, α, β) with varying populations. For simplicity, the system grid will always be a 2-dimensional lattice of equal lengths. Also, the spatial configuration used will be $\theta = \pi$. The total population sample will be perfect squares ranging from 10^1 to 10^4.

For this case, each iteration is considered 1 second. Five trials were performed per sample population. Due to insufferable run times, if a parameter set (a, b, α, β, N) returned a trial with applause duration greater than 60 seconds, it is marked as 0 seconds and no further trials are performed. This means that graphs with data points of 0 seconds are to be disregarded.

Shown in figure 4.4 is the parameter set $(a = 1, b - 0.7, \alpha = 0.8, \beta = 1)$ that best recreates the real-life applause. This was found by simply generating the applause duration versus audience size graph for every parameter set, then comparing

its fitting function with that of the real applause. Similar parameter sets are shown in the appendix (G) Though this is the best fit parameter set, it still does not fully emulate the real applause. As seen, the data points for the real-life applause is more deviant compared to the simulation. The model may still be incomplete, or the data points for real-life applause is not enough. On reason for this is that the data points for real applause is not enough. Data acquisition was difficult due to a duration-size uncertainty. For big audience sizes, the size is well defined because of the seating capacity of the stadium or the ticket sales for the event. Applause duration is very uncertain because it is very hard to determine when the applause starts and ends due to the sheer amount of people. Also, at no point does the crowd go completely silent, making it hard to distinguish applause from cheers and screems. For small audience sizes, the applause is well defined since it is clearly audible in the video, and can also be visually confirmed. The audience size is uncertain because the videos of small audience sizes are either street performances or room performances. For street perfomances, people come and go. For room performances, the videographer is focused on the performer, thus the audience size cannot be confirmed with absolute certainty and must be estimated. Another source for error is the spatial configuration. The given setup only accounts for sight. A box with the reference agent at the center can be added in order to account for audible influence. Finally, the assumption that everyone claps after the performance does not encapsulate all forms of audience applause. This aspect can included by varying the forcing function to different probabilities, instead of 100An in-depth analysis on the new model is also warranted.

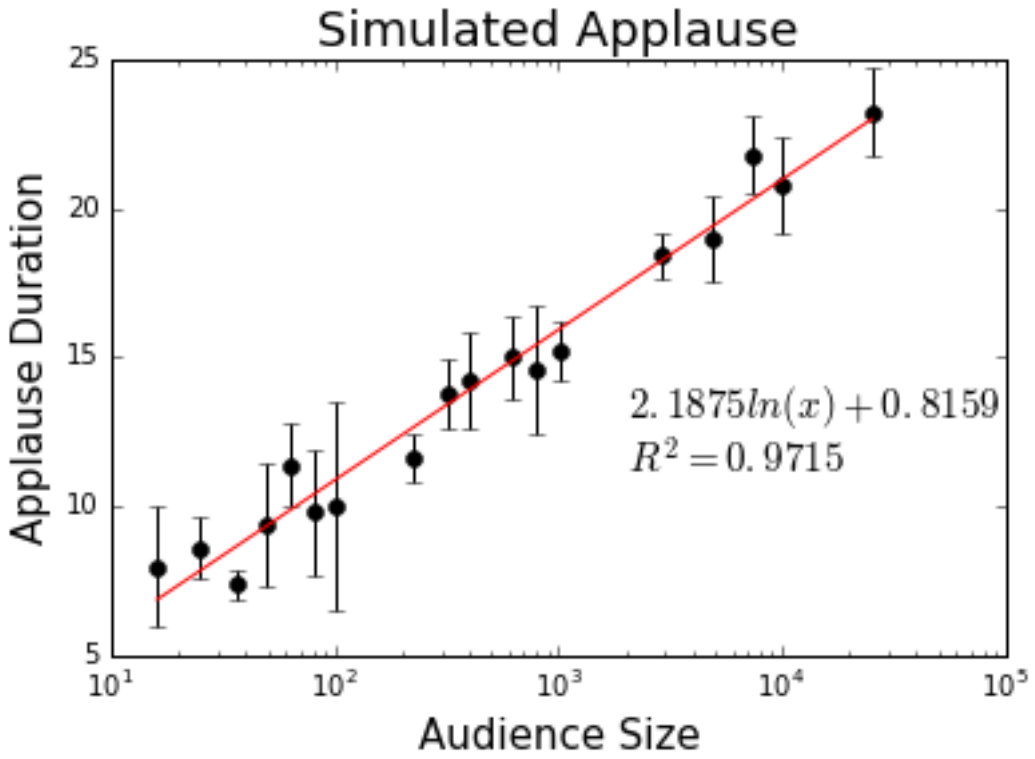

(a) Simulated points showing population size dependence.

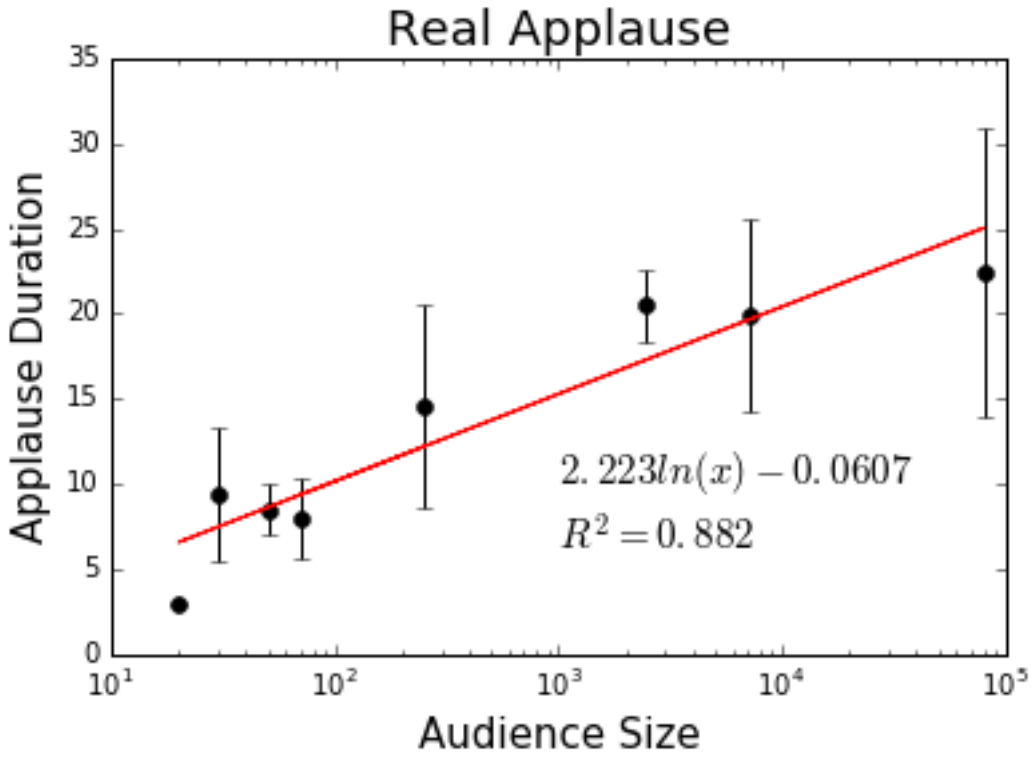

(b) Real-life data points on population size dependence.

Figure 4.4: Comparing the simulated and actual graph of applause duration versus population size. Both increase linearly in the logarithmic scale.

Chapter 5

Conclusions and Recommendations

A compartmental model SIS-like model was successfully constructed to study the complexity of the audience applause, as well as simulate it with an agent-based Monte Carlo method. The original, fully-connected system exhibited parameter sets that express a non-trivial steady-state solution. The dynamics of the given system were studied, uncovering critical points in the phase space plot. These critical points provide the point at which the model bifurcates from the trivial steady-state solution to the non-trivial stready-state solution. For $\beta \leq 1$, the critical point is $\bar{a}_1 \approx b$. The system follows the trivial solution for $\bar{a} \leq \bar{a}_1$ and then bifurcates at the critical point. After which, it follows the non-trivial solution. For $\beta > 1$, there is a second critical point $\bar{a}_2 = \frac{b(N-1)^2}{(N-n_c^*)(N-1+\beta n_c^*)}$ where $n_c^* \equiv [1 + (\beta - 1)N]/2\beta$. The system follows the trivial solution for $\bar{a} \leq \bar{a}_2$ and then bifurcates somewhere before critical point. Bifurcation for parameter sets with $\beta > 1$ are only partially predicted. Once it bifurcates to the non-trivial steady-state, it follows the upper branch of the curve. Also, the lower branch of $\beta > 1$ curves are shown to be unstable; if the system starts with a state n_c on the lower branch, it can either settle to the trivial or non-trivial solution. Further modifications were made to the compartmental model in order to incorporate spatial effects, as such effects more closely resembled a real-life applause. Three spatial configurations were investigated, $\theta = 0, \frac{\pi}{2}, \pi$, each θ value corresponding to the view of the reference agent. Each configuration successfully incorporated the population size dependence of the applause duration. $\theta = \pi$ was used as it was the most realistic as well as the easiest to implement in code. This allowed simulations to show a correlation between applause duration and audience size. The simulations were backed by data points of real-life applause. Analysis of the model with incorporated spatial effects is necessary in order to understand the

dynamics of the audience applause. This will allow further development of the model, which in turn, will more closely resemble the real-life applause.

Appendix A

Combined probability of functions f and f'

The forcing function f permits agents to undergo R_1 and is represented with a probability p_1. The probability that R_1 does not occur is $q_1 = 1 - p_1$. Likewise for the function f' to undergo R_1 is represented with a probability p_2, and non-occurring probability q_2. Combining the probabilities p and q results to

$$p_1 + q_1 = 1 \tag{A.1}$$

$$p_2 + q_2 = 1 \tag{A.2}$$

Multiplying the equations (A.1) and (A.2) and simplifying

$$(p_1 + q_1)(p_2 + q_2) = 1 \tag{A.3}$$

$$p_1p_2 + p_1q_2 + p_2q_1 + q_1q_2 = 1 \tag{A.4}$$

q_1q_2 represents neither event occuring thus

$$p_{net} = 1 - q_1q_2 = 1 - (1 - p_1)(1 - p_2) \tag{A.5}$$

$$= 1 - (1 - p_1 - p_2 + p_1p_2) \tag{A.6}$$

$$= p_1 + p_2 - p_1p_2 \tag{A.7}$$

Replacing (A.7) with the functions gives

$$p_{net} = f + f' - f'f \tag{A.8}$$

which is used in (2.7)

Appendix B

Deriving the steady-state equation

Setting $\frac{d\vec{n}}{dt} = 0$,

$$\frac{d}{dt}n_c = 0 \tag{B.1}$$

$$a(f + f' - f'f)n_s - bg'n_c = 0 \tag{B.2}$$

$$a(f + f' - f'f)n_s = bg'n_c \tag{B.3}$$

$$\tag{B.4}$$

Note: $N = n_c + n_s, n_s = N - nc$, and $f = 0$.

$$af'(N - nc) = bg'n_c \tag{B.5}$$

Plugging in (2.3) and (2.4) to (B.5):

$$a(\alpha\frac{n_c}{N-1})(N - n_c) = b(\frac{1}{1 + \frac{\beta n_c}{N-1}})(n_c) \tag{B.6}$$

$$\frac{a\alpha(N - n_c)}{N-1}n_c = b\frac{N-1}{N-1+\beta n_c}n_c \tag{B.7}$$

$$a\alpha(N - n_c) = b\frac{(N-1)^2}{N-1+\beta n_c} \tag{B.8}$$

$$a\alpha(N - n_c)(N - 1 + \beta n_c) = b(N-1)^2 \tag{B.9}$$

Appendix C

Steady-state Phase Space

Shown are the phase space plots for various b values.

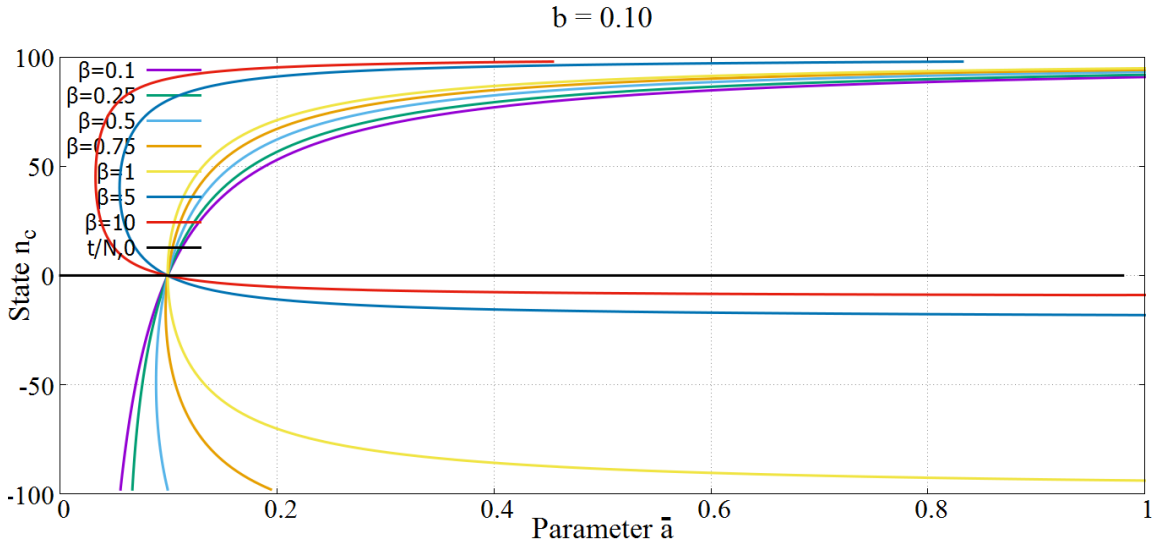

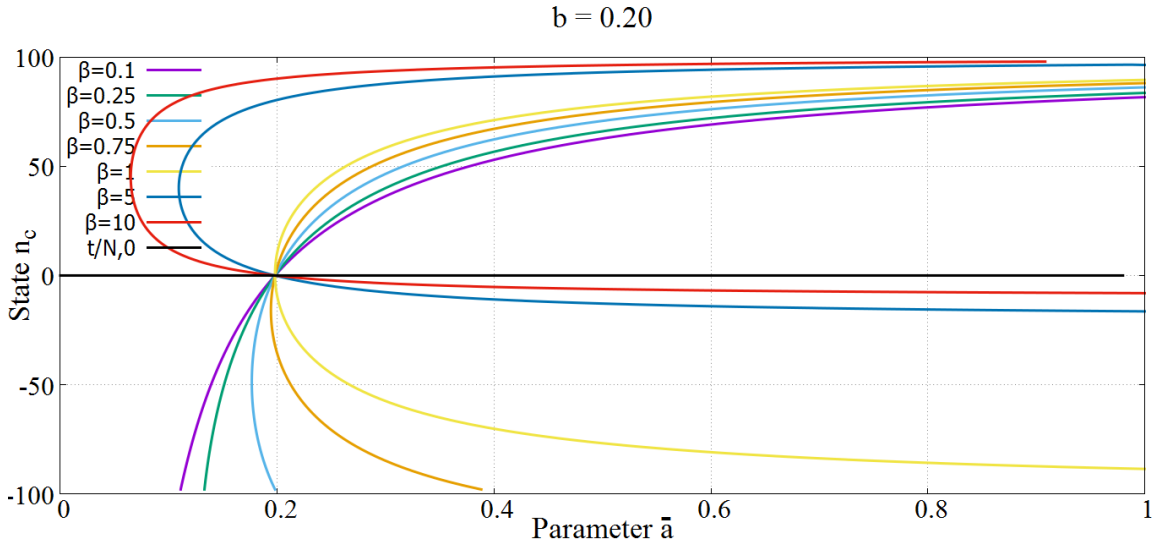

b = 0.30

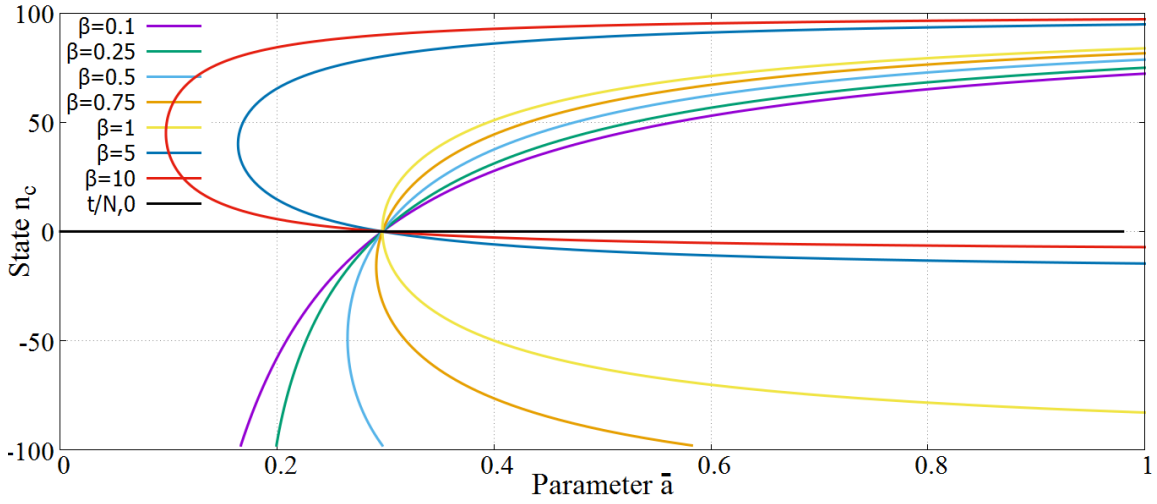
β=0.1
β=0.25
β=0.5
β=0.75
β=1
β=5
β=10
t/N,0
State n_c
Parameter ā
100
50
0
-50
-100
0
0.2
0.4
0.6
0.8
1

b = 0.40

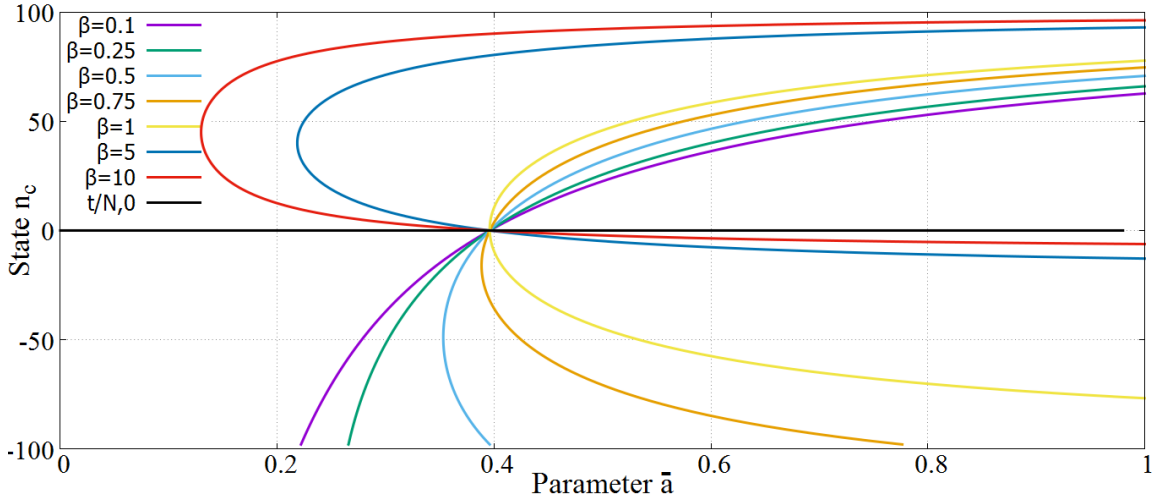
β=0.1
β=0.25
β=0.5
β=0.75
β=1
β=5
β=10
t/N,0
State n_c
Parameter ā
100
50
0
-50
-100
0
0.2
0.4
0.6
0.8
1

b = 0.50

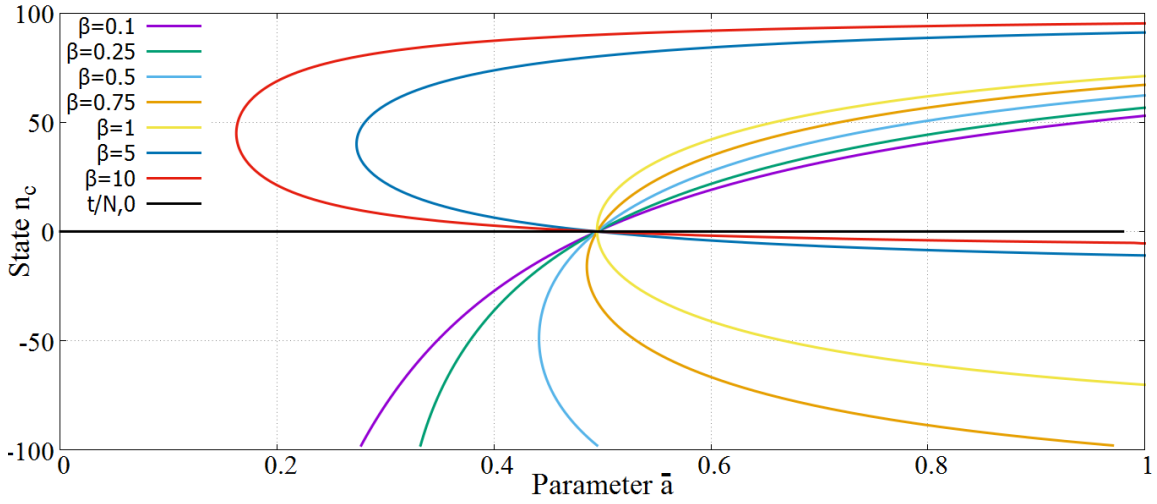
β=0.1
β=0.25
β=0.5
β=0.75
β=1
β=5
β=10
t/N,0
State n_c
Parameter ā
100
50
0
-50
-100
0
0.2
0.4
0.6
0.8
1

b = 0.60

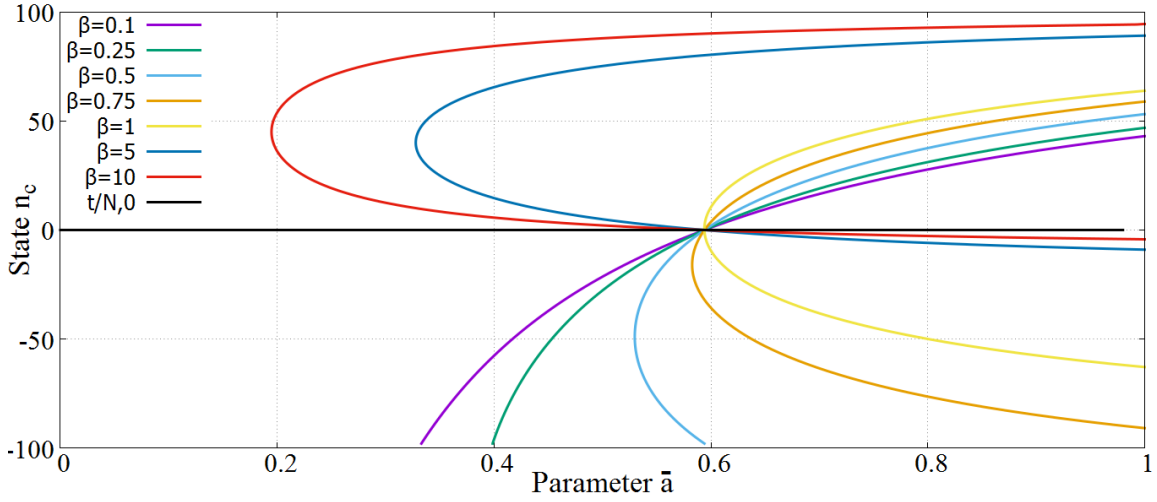
β=0.1
β=0.25
β=0.5
β=0.75
β=1
β=5
β=10
t/N,0
State n_c
Parameter ā
100
50
0
-50
-100
0
0.2
0.4
0.6
0.8
1

b = 0.70

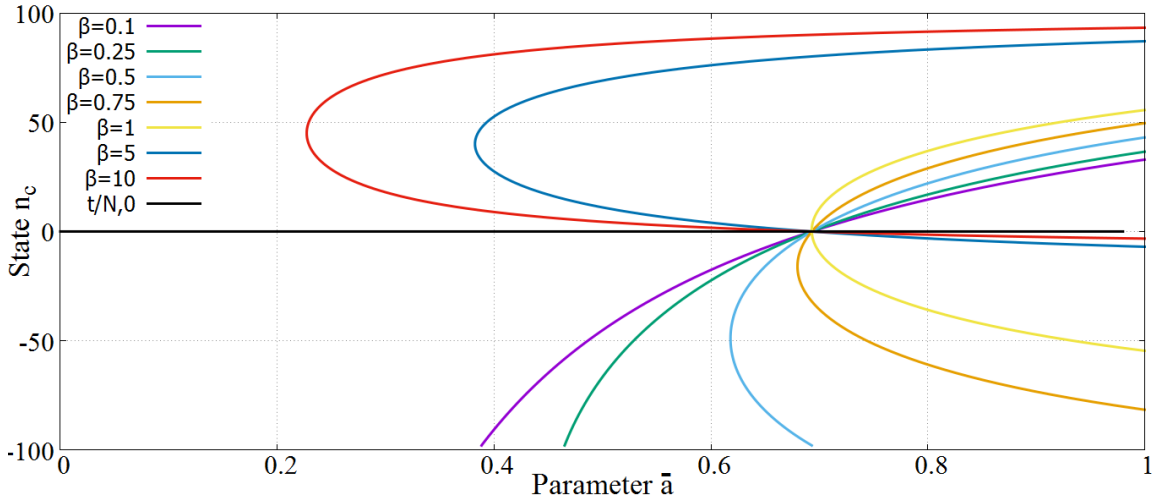
β=0.1
β=0.25
β=0.5
β=0.75
β=1
β=5
β=10
t/N,0
State n_c
Parameter ā
100
50
0
-50
-100
0
0.2
0.4
0.6
0.8
1

b = 0.80

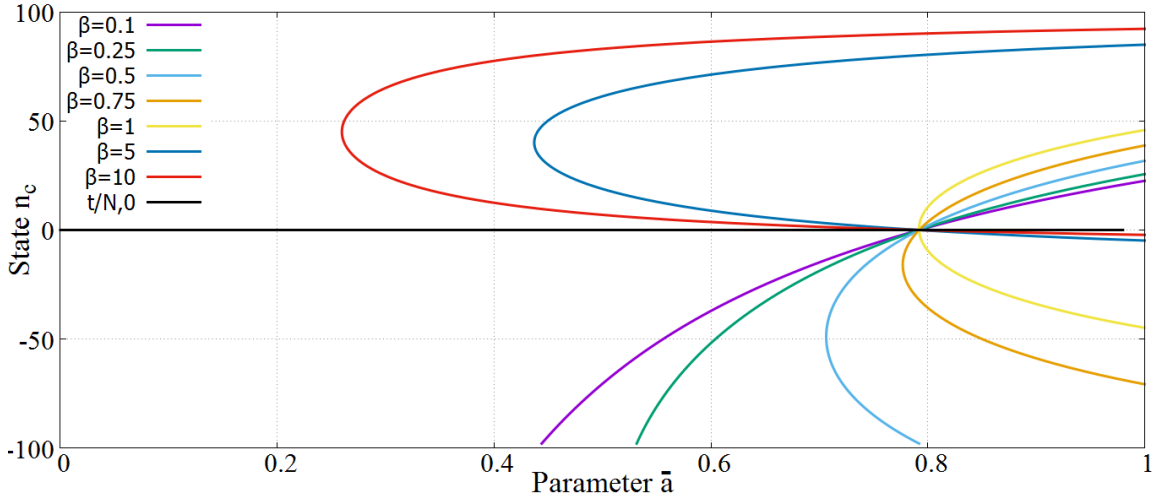
β=0.1
β=0.25
β=0.5
β=0.75
β=1
β=5
β=10
t/N,0
State n_c
Parameter ā
100
50
0
-50
-100
0
0.2
0.4
0.6
0.8
1

b = 0.90

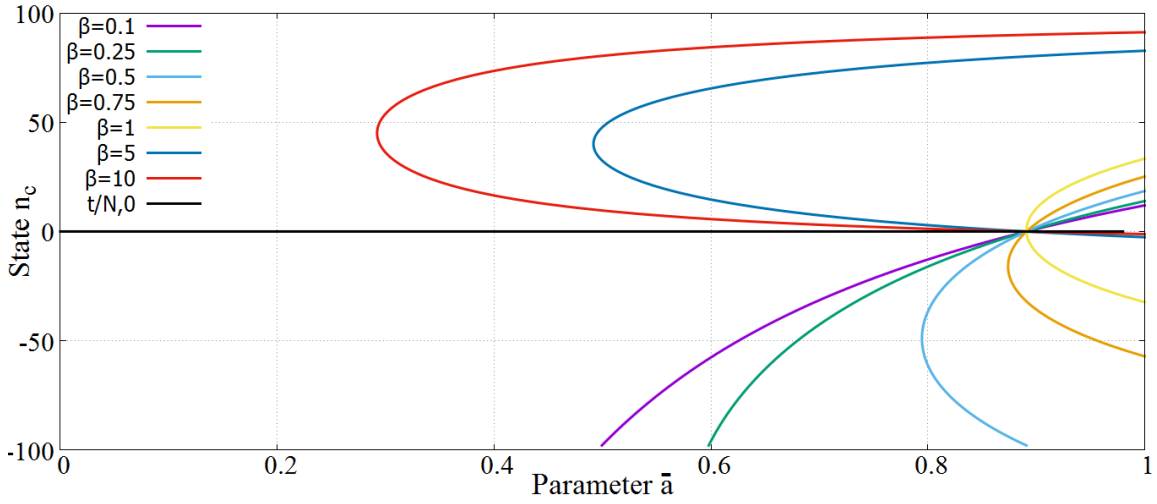
β=0.1
β=0.25
β=0.5
β=0.75
β=1
β=5
β=10
t/N,0
100
50
0
-50
-100
State n_c
0
0.2
0.4
0.6
0.8
1
Parameter ā

b = 1.00

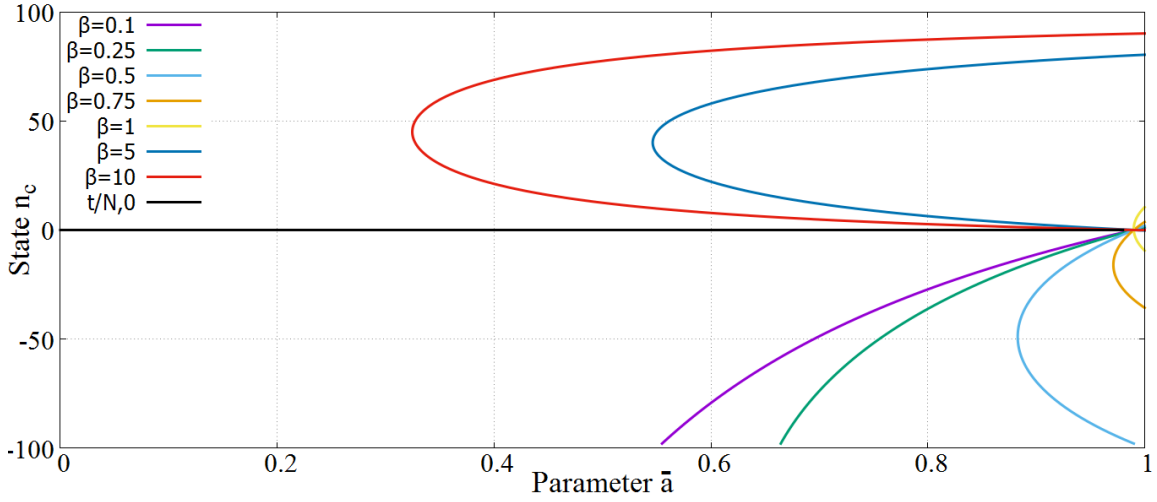
β=0.1
β=0.25
β=0.5
β=0.75
β=1
β=5
β=10
t/N,0
100
50
0
-50
-100
State n_c
0
0.2
0.4
0.6
0.8
1
Parameter ā

Appendix D

Critical points

Setting $n_c = 0$ in the steady-state equation (3.1) gives us this critical point of intersection

$$\bar{a}(N - n_c)(N - 1 + \beta n_c) = b(N-1)^2 \tag{D.1}$$

$$\bar{a}N(N-1) = b(N-1)^2 \tag{D.2}$$

$$\bar{a} = \frac{b(N-1)^2}{N(N-1)} \tag{D.3}$$

$$\bar{a}_1 = \frac{b(N-1)}{N} \tag{D.4}$$

$$\tag{D.5}$$

On the other hand, $\bar{a_2}$ is arrived by plugging in a special n_c value, $n_c^* \equiv [1 + (\beta - 1)N]/2\beta$.

$$\bar{a}(N - n_c^*)(N - 1 + \beta n_c^*) = b(N-1)^2 \tag{D.6}$$

$$\bar{a}_2 = \frac{b(N-1)^2}{(N - n_c^*)(N - 1 + \beta n_c^*)} \tag{D.7}$$

Appendix E

Steady-state Simulations Results

Shown are the phase space plots along with the simulated data points using the same parameters for various b and β values.

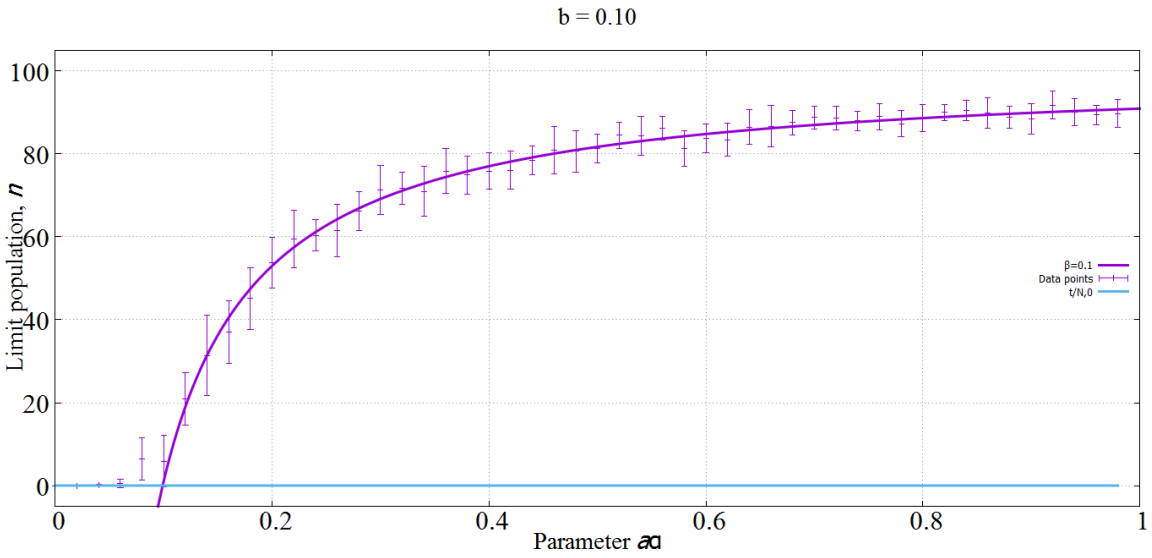

b = 0.10

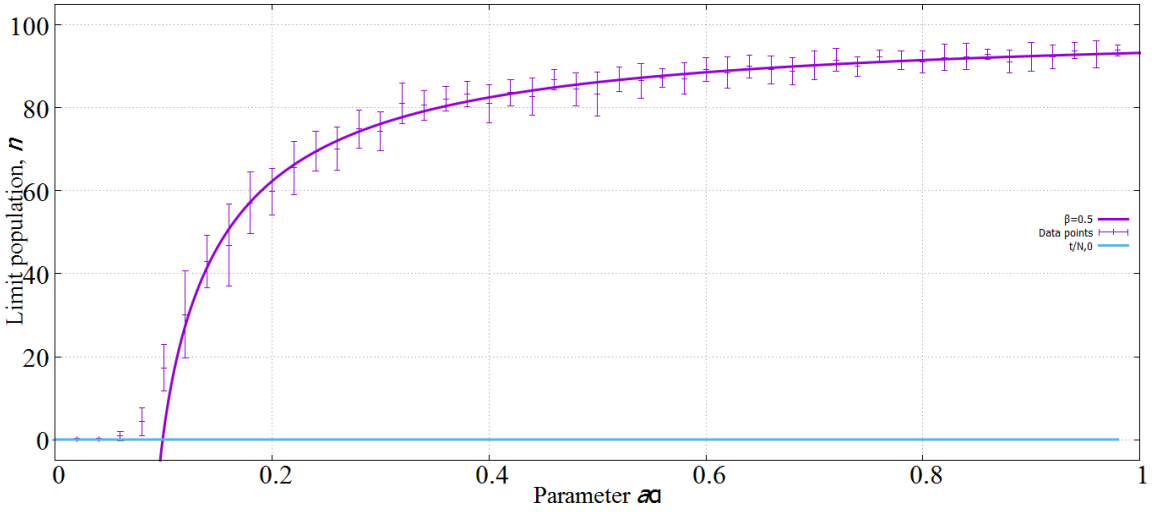

b = 0.10

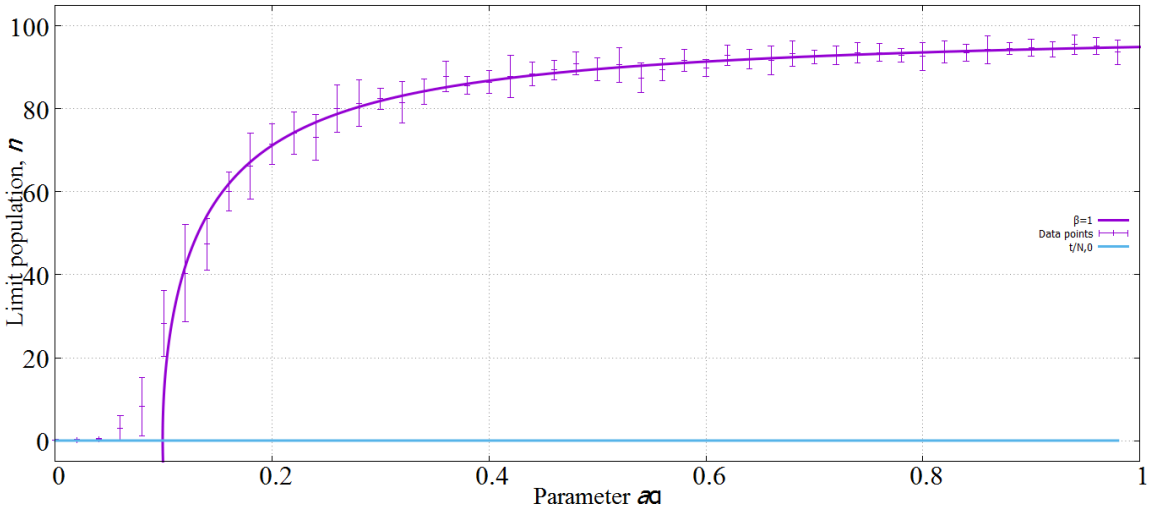

b = 0.10

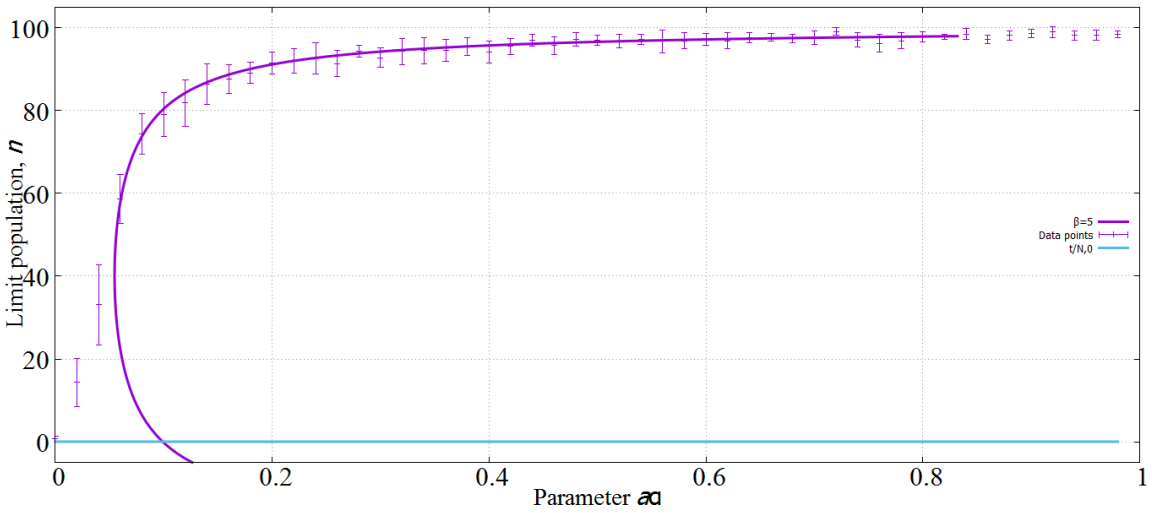

b = 0.10

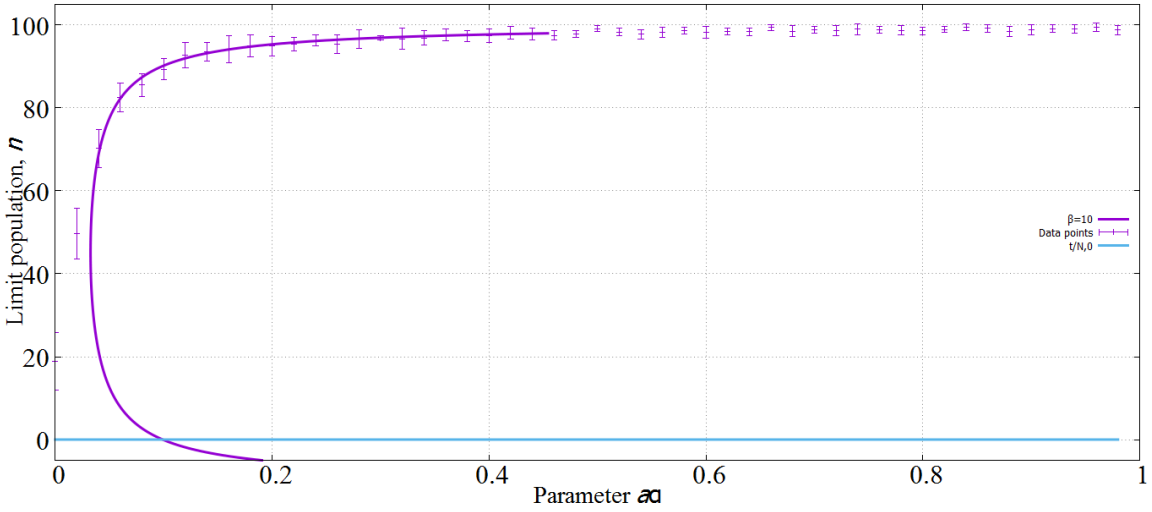

b = 0.50

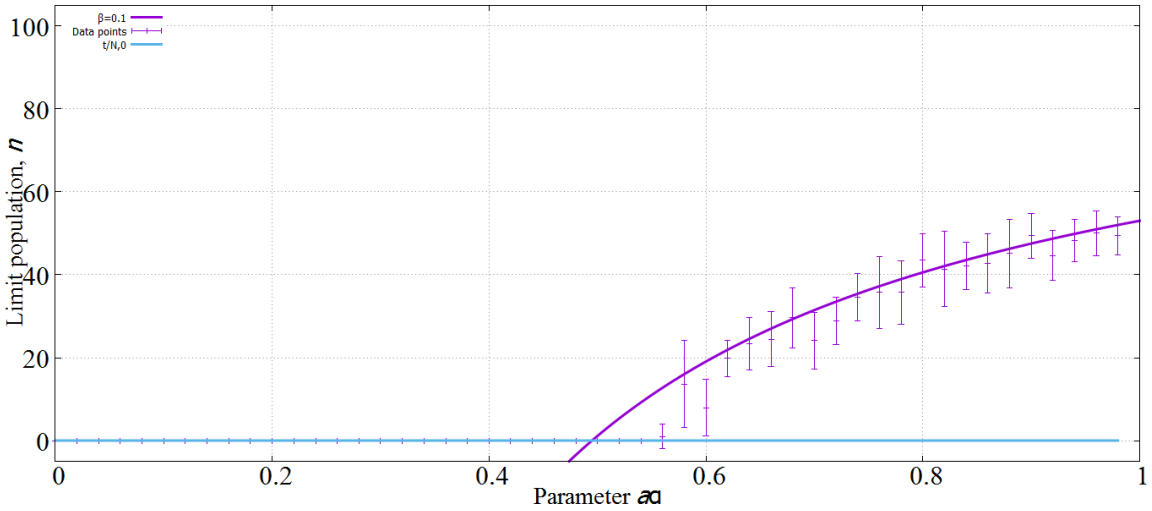

b = 0.50

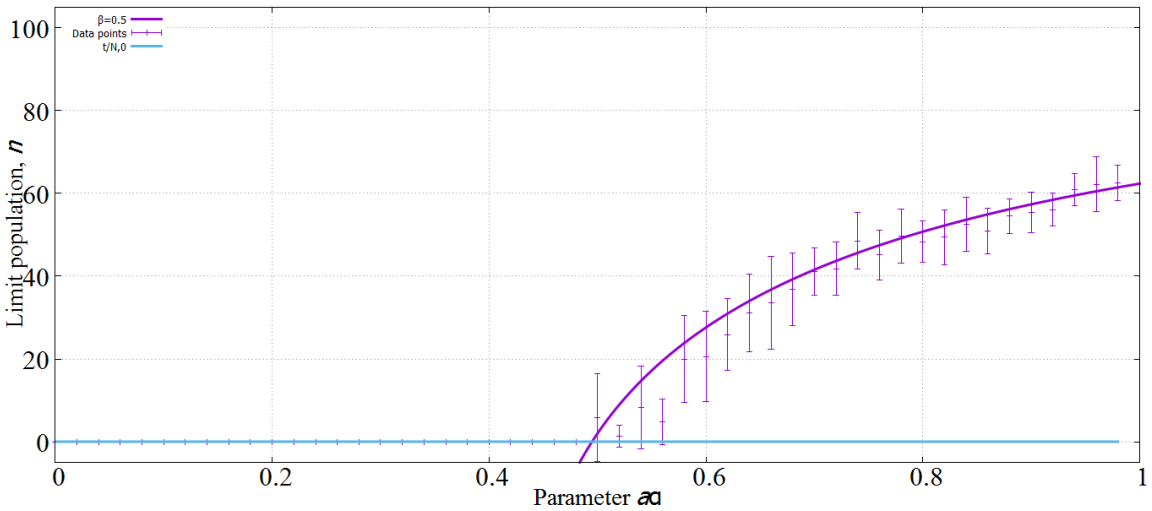

b = 0.50

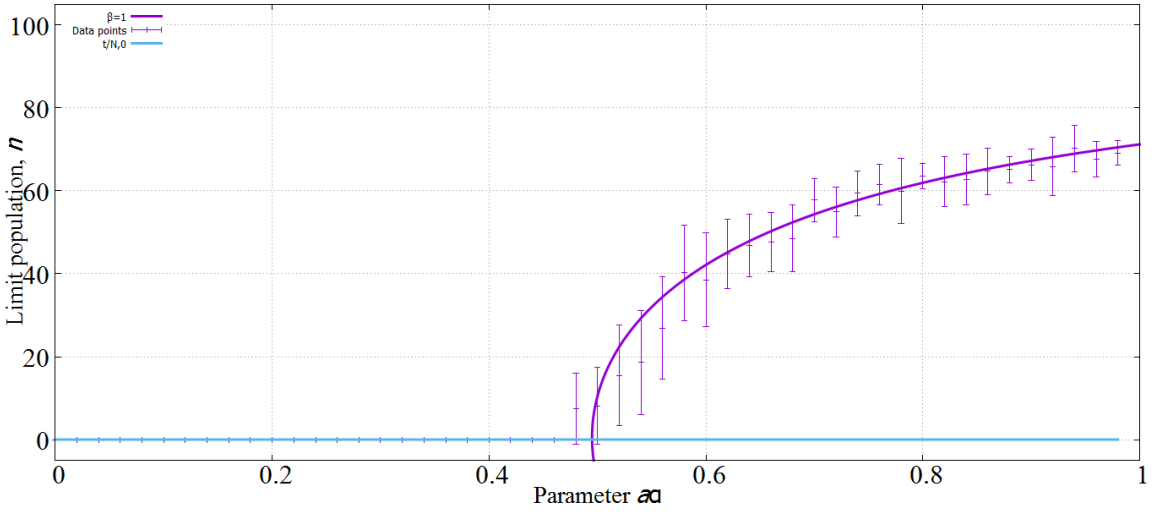

b = 0.50

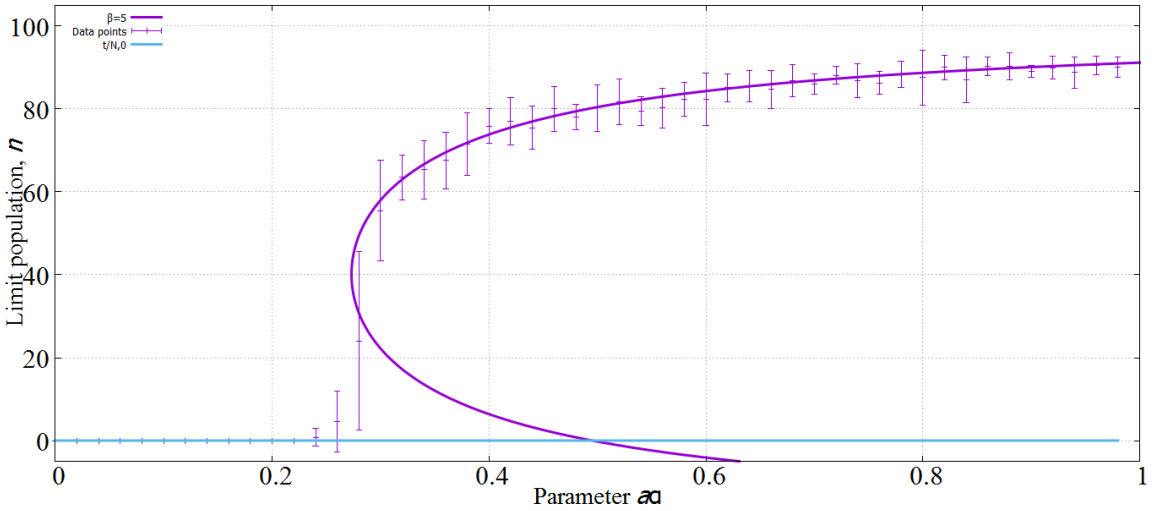

b = 0.50

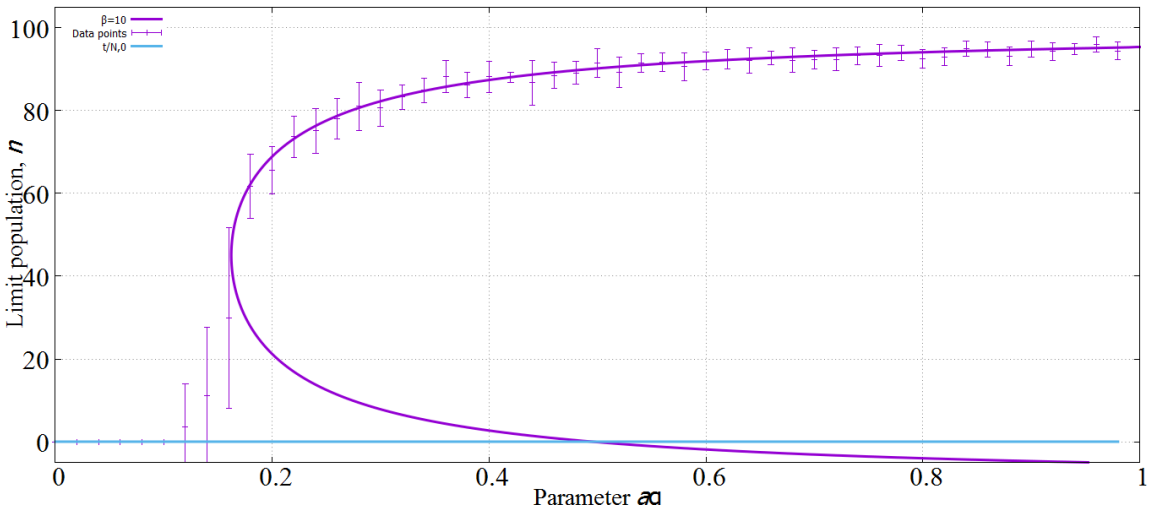

b = 0.80

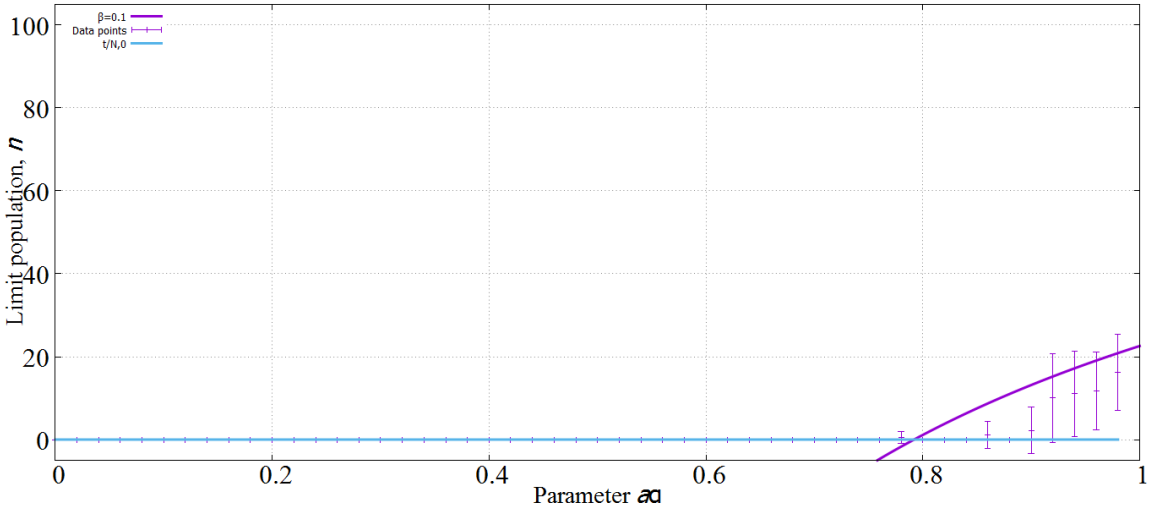

b = 0.80

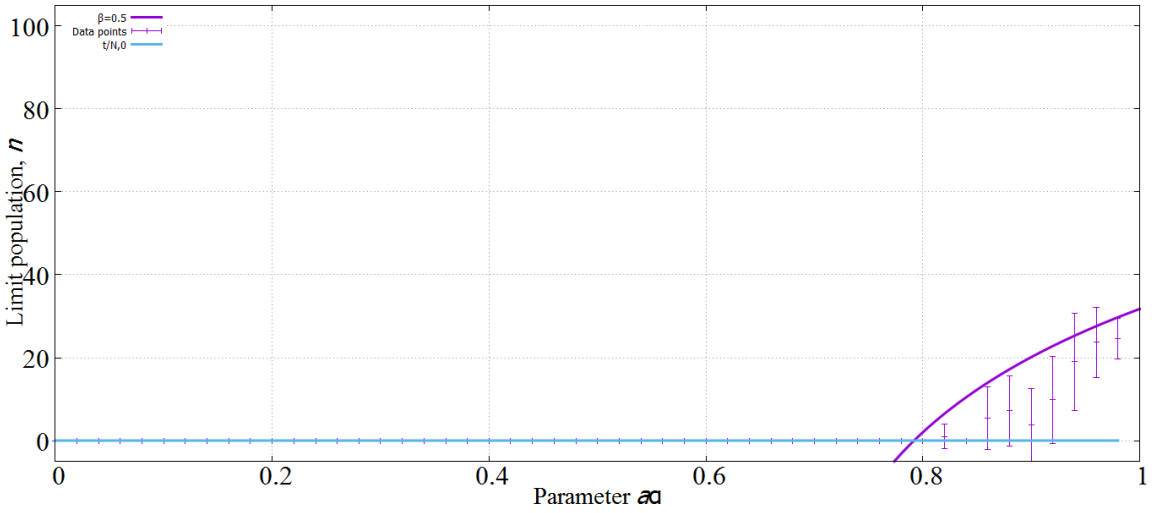

b = 0.80

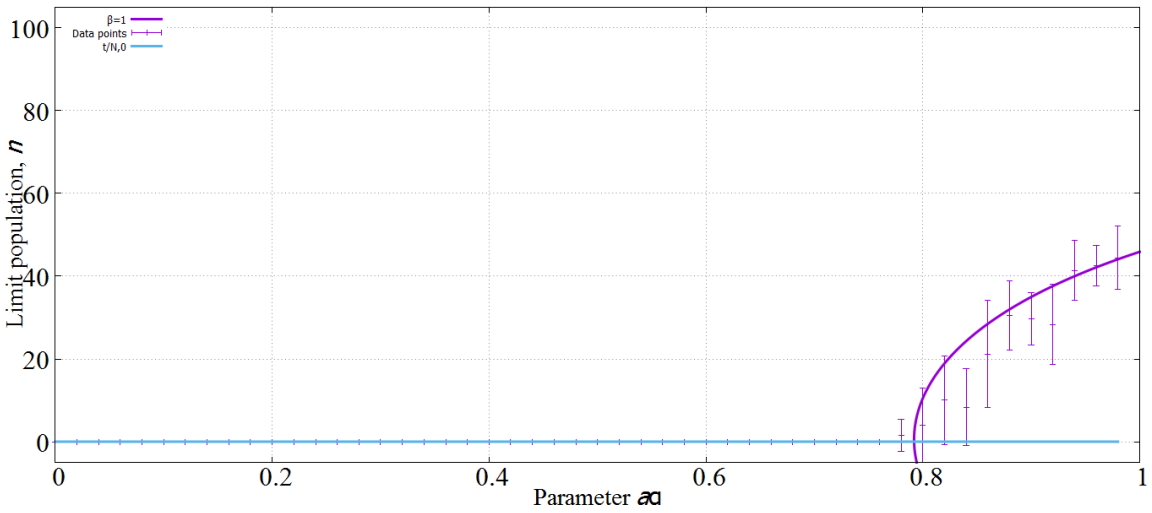

b = 0.80

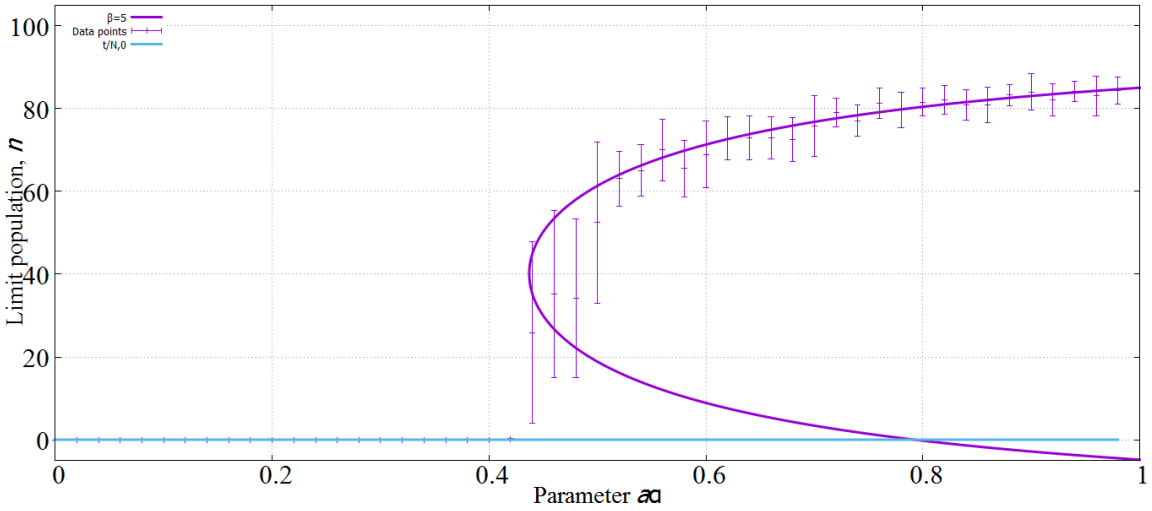
β=5
Data points
t/N,0
Limit population, n
Parameter a
0
20
40
60
80
100
0
0.2
0.4
0.6
0.8
1

b = 0.80

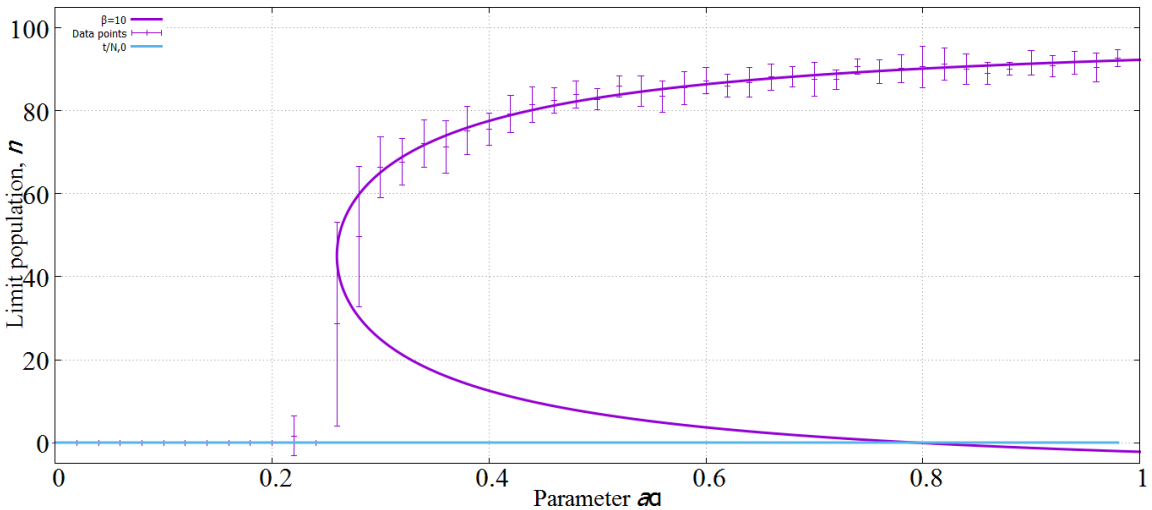
β=10
Data points
t/N,0
Limit population, n
Parameter a
0
20
40
60
80
100
0
0.2
0.4
0.6
0.8
1

Appendix F

Vector Graphs

Shown are the phase space plots along with probabilistic vectors pointing towards the steady-state for various b and β values.

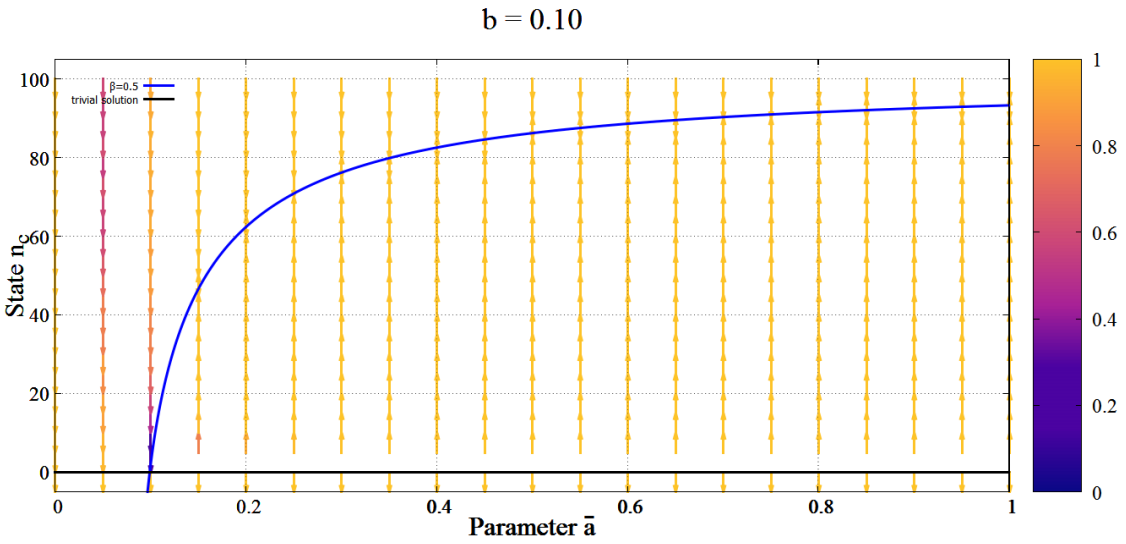

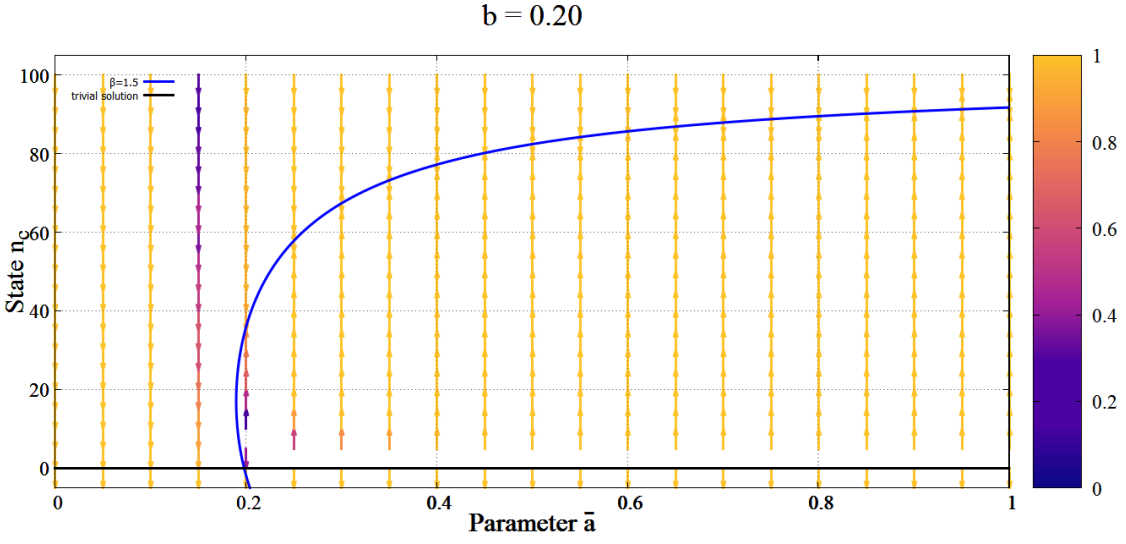

b = 0.40

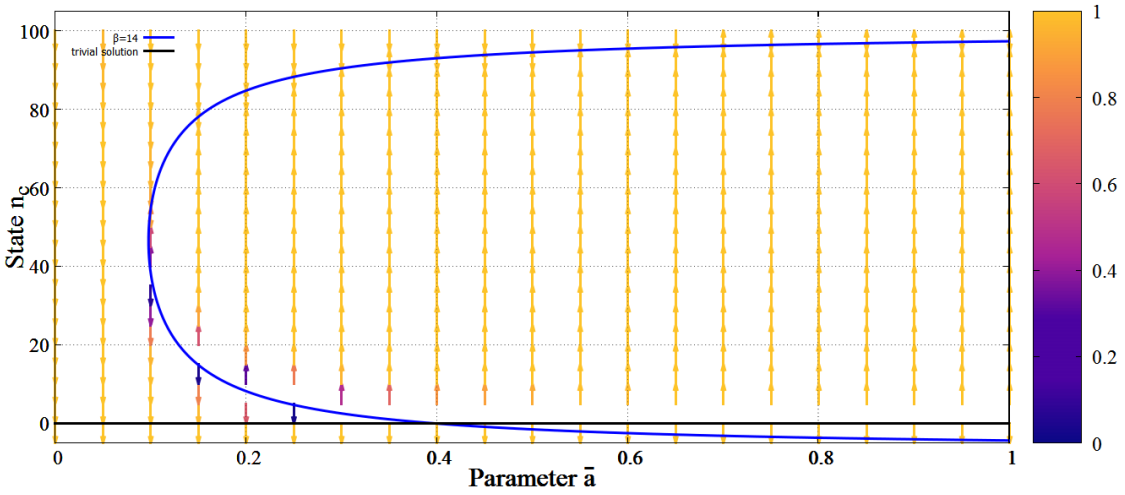
β=14
trivial solution
State n_C
Parameter ā
0
20
40
60
80
100
0.2
0.4
0.6
0.8
1

b = 0.90

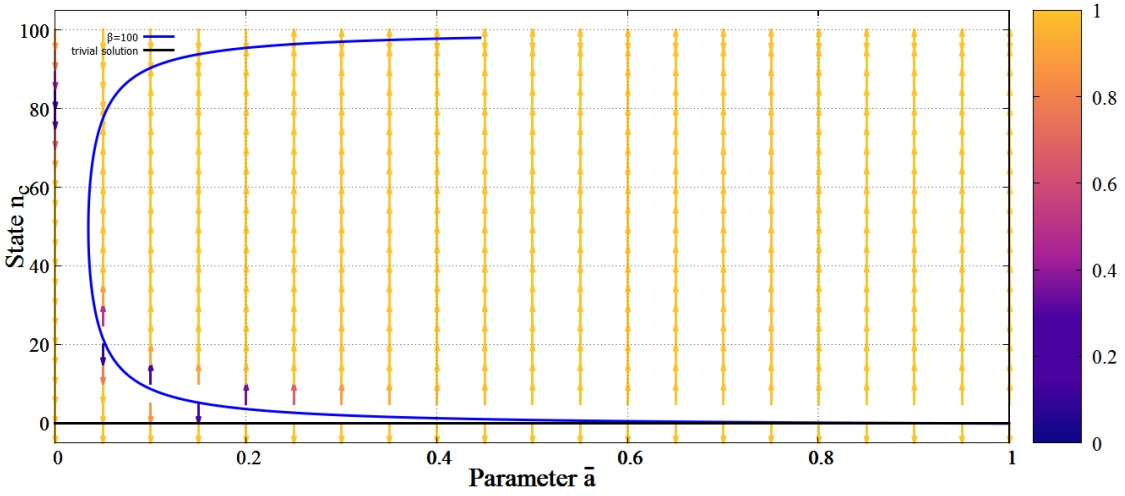
β=100
trivial solution
State n_C
Parameter ā
0
20
40
60
80
100
0.2
0.4
0.6
0.8
1

Appendix G

Best fit parameter sets

Shown are the graphs of applause duration versus population size of parameter sets that closely resemble the real-life data points.

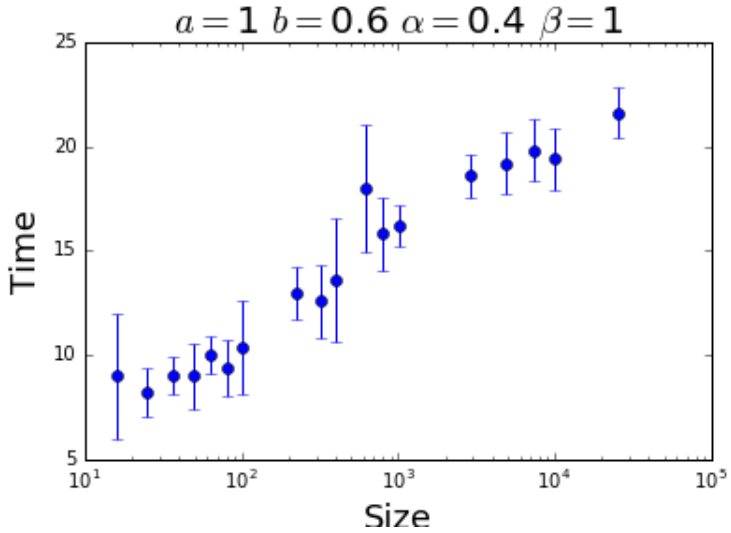

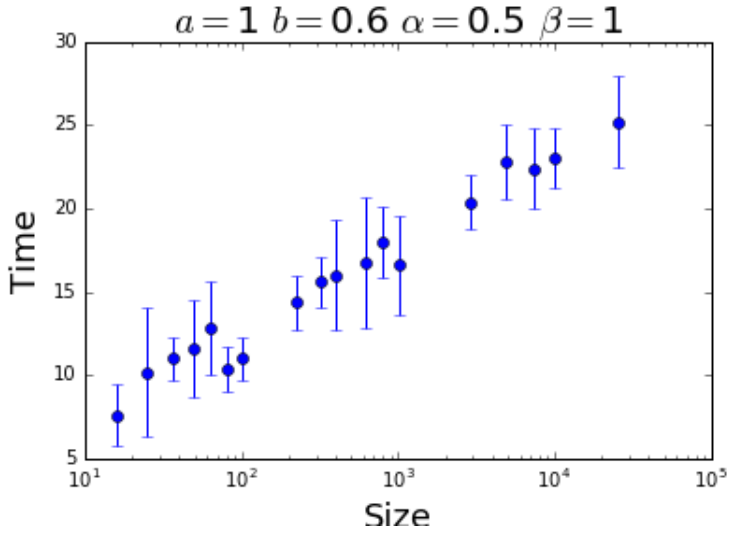

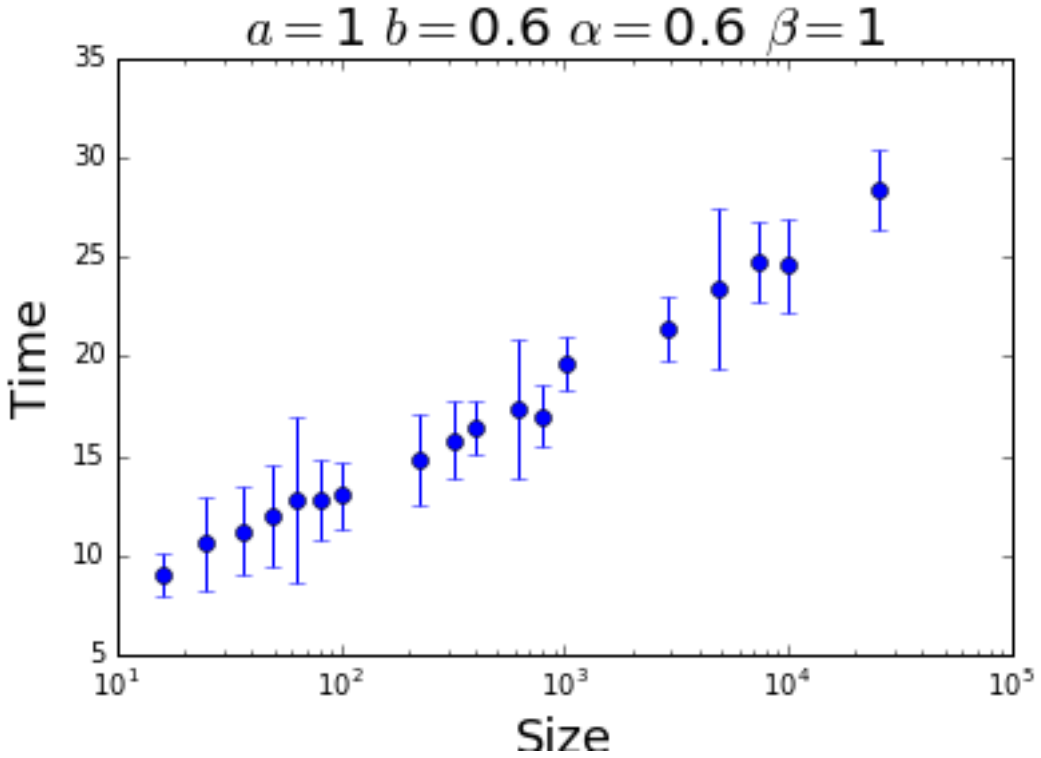
$a = 1$ $b = 0.6$ $\alpha = 0.6$ $\beta = 1$
Time
Size
35
30
25
20
15
10
5
10^1
10^2
10^3
10^4
10^5

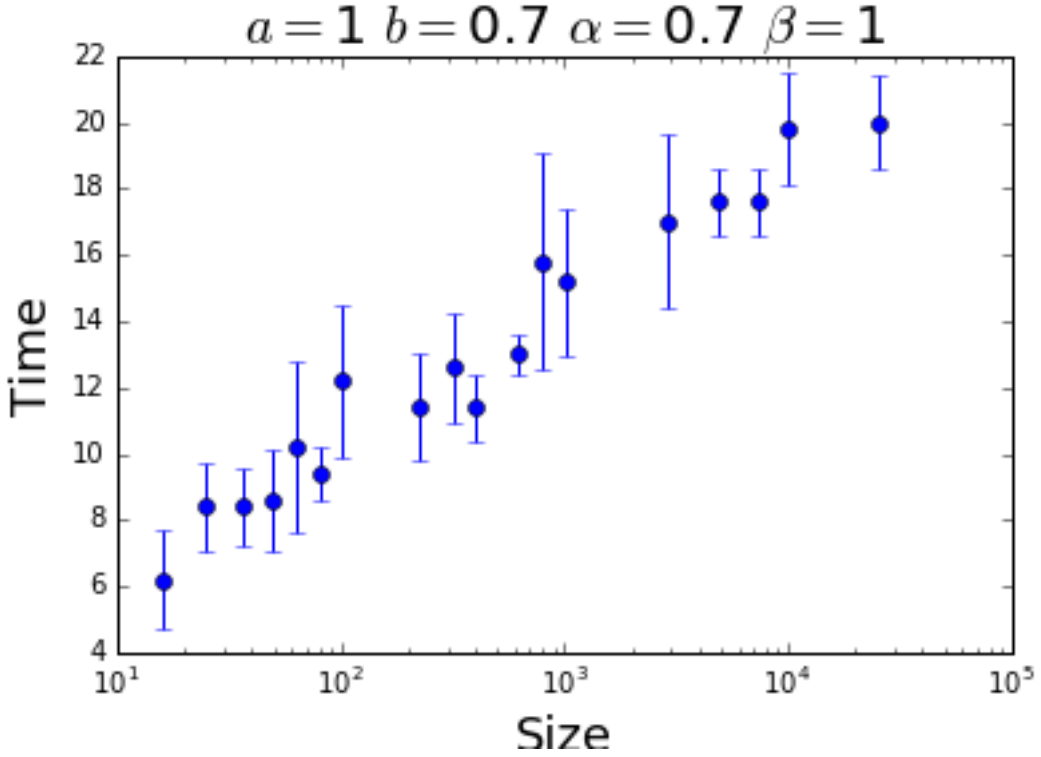
$a = 1$ $b = 0.7$ $\alpha = 0.7$ $\beta = 1$
Time
Size
22
20
18
16
14
12
10
8
6
4
10^1
10^2
10^3
10^4
10^5

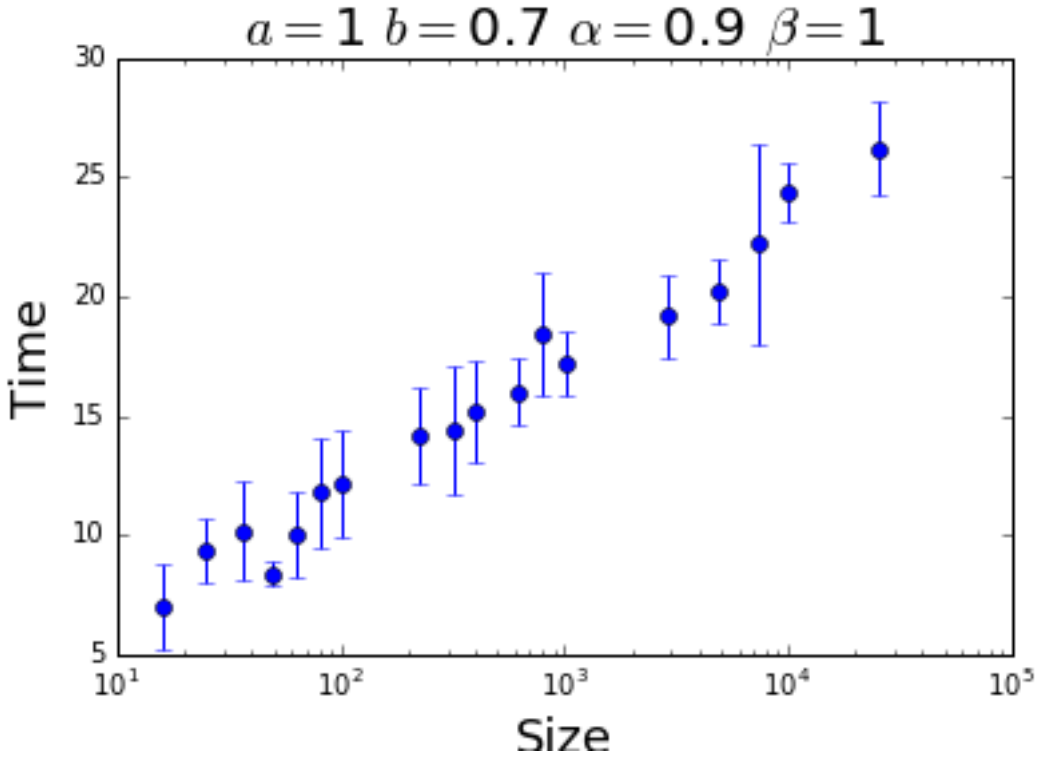
$a = 1$ $b = 0.7$ $\alpha = 0.9$ $\beta = 1$
Time
Size
30
25
20
15
10
5
10^1
10^2
10^3
10^4
10^5

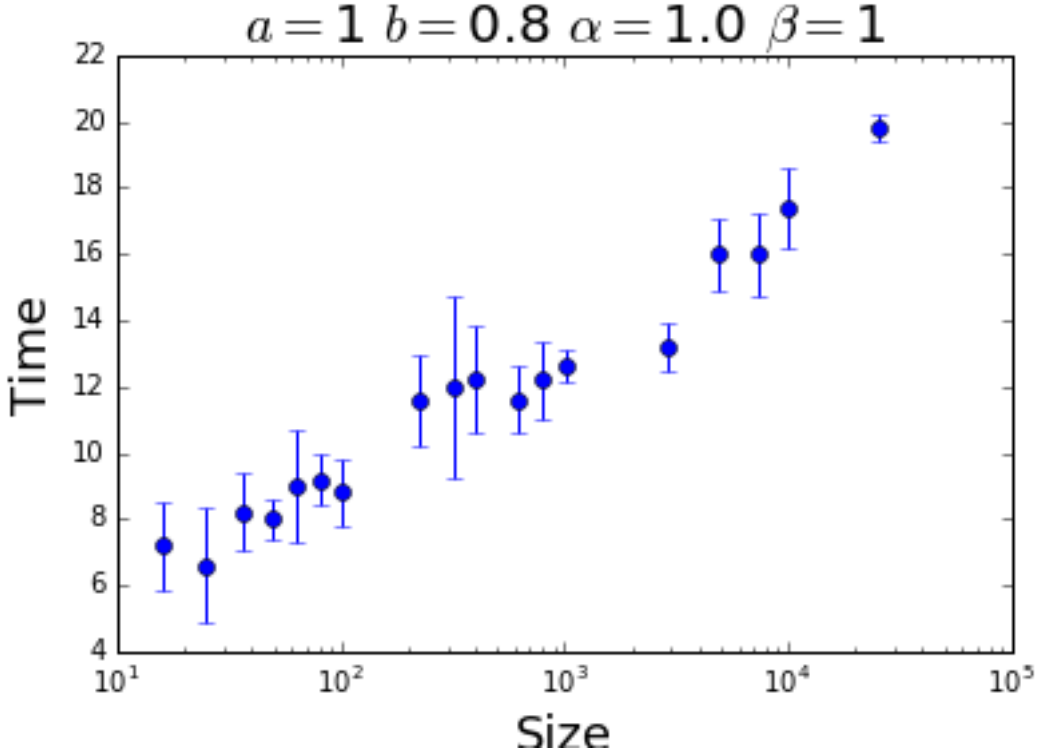
$a = 1$ $b = 0.8$ $\alpha = 1.0$ $\beta = 1$
Time
Size
22
20
18
16
14
12
10
8
6
4
10^1
10^2
10^3
10^4
10^5

Bibliography

[1] B. Howarth, "Origins of the claque in the french theatre," *OUP Academic*, Oct 1999.

[2] S. Durlauf and H. P. Young, *Social Dynamics (Economic Learning and Social Evolution)*, vol. 1. Academic Press, 2001.

[3] B. Krauth, "Simulation-based estimation of peer effects," *Journal of Econometrics*, vol. 133, no. 0304-4076, pp. 243–271, 2006.

[4] M. Newman, *Networks: An Introduction*. Oxford University Press, 2010.

[5] S. N. Dorogovtsev and J. Mendes, *Evolution of Networks: From Biological Nets to the Internet and WWW (Physics)*. Oxford University Press, 2003.

[6] P. Bak, *How Nature Works: the science of self-organized criticality*. Copernicus, 1999.

[7] T. S. Deisboeck and J. Yasha Kresh, eds., *Complex Systems Science in Biomedicine (Topics in Biomedical Engineering. International Book Series)*. Springer, 2006.

[8] R. Albert and A.-L. Barabási, "Statistical mechanics of complex networks," *Rev. Mod. Phys.*, vol. 74, pp. 47–97, Jan 2002.

[9] L. J. Gray, "A mathematician looks at wolfram's new kind of science, volume 50, number 2," 2002.

[10] Z. Nda, E. Ravasz, Y. Brechet, T. Vicsek, and A.-L. Barabsi, "The sound of many hands clapping," *Nature*, vol. 403, no. 6772, p. 849850, 2000.

[11] Z. Nda, E. Ravasz, Y. Brechet, T. Vicsek, and A.-L. Barabsi, "The sound of many hands clapping," *Nature*, vol. 403, no. 6772, p. 849850, 2000.

[12] R. P. Mann, J. Faria, D. J. T. Sumpter, and J. Krause, "The dynamics of audience applause," *Journal of The Royal Society Interface*, vol. 10, no. 85, 2013.

[13] e. a. J. Arino, F. Brauer, "Simple models for containment of a pandemic," *Journal of The Royal Society Interface*, vol. 3, no. 8, pp. 453–457, 2006.

[14] K. A. Johnson and R. S. Goody, "The original michaelis constant: Translation of the 1913 michaelismenten paper," *Biochemistry*, vol. 50, p. 82648269, Apr 2011.

[15] K. T.-A. A. Champneys, *Dynamical Systems Theory, Bifurcation Analysis*, pp. 632–637. New York, NY: Springer New York, 2013.